stimulation of the inflammatory response by induction of production of proinflammatory cytokines and chemokines, oxidative molecules induce pulmonary cell apoptosis, activate proteases, and inactivate antiproteases (Valentin et al., 2005; Rahman and Adcock, 2006; Greenlee et al., 2007).

Superoxide dismutase (SOD) catalyzes the dismutation of superoxide anion to hydrogen peroxide, which is subsequently detoxified to oxygen and water (Kinnula and Crapo, 2003). Of human SODs, Cu/Zn-SOD accounts for 80% of all SOD activities within the lung (Kinnula and Crapo, 2003). Altered levels of expression and activity of SOD were observed in both patients with COPD and animals treated with elastase or CS (animal models for COPD) (Kondo et al., 1994; Daga et al., 2003; Valenca et al., 2008), and transgenic mice expressing Cu/Zn-SOD were resistant to elastase- or CS-induced pulmonary emphysema (Foronjy et al., 2006). Furthermore, transgenic mice expressing another type of SOD, extracellular SOD, or knockout mice for this protein were resistant or sensitive, respectively, to elastase- or CS-induced pulmonary emphysema through attenuating oxidative fragmentation of extracellular matrix (Yao et al., 2010). These results suggest that administration of SOD could be of therapeutic benefit in the treatment of COPD. However, because of its low affinity for tissues and low stability in plasma, there is no report showing that administration of SOD is effective for the treatment of patients with COPD or elastase- or CS-induced pulmonary emphysema in animals.

Igarashi et al. (1992) developed PC-SOD, a lecithinized human Cu/Zn-SOD in which four phosphatidylcholine (PC) derivative molecules are covalently bound to each SOD dimer. This modification drastically improves the plasma stability and cellular affinity of SOD (Igarashi et al., 1992,1994; Ishihara et al., 2009). As described under *Discussion*, clinical studies showed that intravenously administered PC-SOD is effective for ulcerative colitis and idiopathic pulmonary fibrosis (IPF) (Broeyer et al., 2008; Suzuki et al., 2008a,b) Furthermore, we recently reported that inhalation of PC-SOD is effective against bleomycin-induced pulmonary fibrosis in mice (an animal model for IPF) (Tanaka et al., 2010). We believe that inhalation may be a viable option for administration of PC-SOD, which would improve the quality of life (QOL) of patients treated with this drug. In this study, we found that inhalation of PC-SOD suppresses elastase-induced pulmonary inflammation, emphysema, and dysfunction, through suppression of cell death, activation of proteases, induction of expression of proinflammatory cytokines and chemokines, and decrease in the level of α1-antitrypsin (an antiprotease). We propose that inhalation of PC-SOD would be therapeutically beneficial for COPD.

Materials and Methods

Chemicals and Animals. Paraformaldehyde and porcine pancreatic elastase (PPE) were obtained from Sigma (St. Louis, MO). Novo-Heparin (5000 units) for injection was from Mochida Pharmaceutical Co. (Tokyo, Japan). Chloral hydrate was from Nacalai Tesque (Kyoto, Japan). Diff-Quik was from the Sysmex Corporation (Kobe, Japan). Terminal deoxynucleotidyl transferase was obtained from TOYOBO (Osaka, Japan). Biotin 14-ATP, Alexa Fluor 488 goat anti-mouse immunoglobulin G, and Alexa Fluor 488 conjugated with streptavidin were purchased from Invitrogen (Carlsbad, CA). Mounting medium for immunohistochemical analysis (VECTASHIELD) was from Vector Laboratories (Burlingame, CA). The RNeasy kit was obtained from QIAGEN (Valencia, CA), the PrimeScript 1st Strand cDNA Synthesis Kit was from TAKARA Bio (Ohtsu, Japan), and the iQ SYBR Green Supermix was from Bio-Rad Laboratories (Hercules, CA). Cytospin 4 was purchased from Thermo Fisher Scientific (Waltham, MA), and Mayer's hematoxylin, 1% eosin alcohol solution, and mounting medium for histological examination (malinol) were from MUTO Pure Chemicals (Tokyo, Japan). Unmodified SOD (5190 U/mg) and PC-SOD (3000 U/mg) were from our laboratory stocks (Igarashi et al., 1992). The α1-antitrypsin ELISA kit was from Immunology Consultants Laboratory (Newberg, OR). ELISA kits for interleukin (IL)-1β and IL-6 were from Thermo Fisher Scientific. ELISA kits for tumor necrosis factor (TNF)-α, macrophage inflammatory protein (MIP)-2, monocyte chemoattractant protein (MCP)-1, and keratinocyte-derived chemokine (KC) were from R&D Systems (Minneapolis, MN). 4,6-Diamino-2-phenylindole (DAPI), diethylenetriamine-*N*,*N*,*N*′,*N*″,*N*″-pentaacetic acid, and 2-diphenylphosphinoyl-2-methyl-3,4-dihydro-2*H*-pyrrole *N*-oxide (DPhPMPO) were from Dojindo (Kumamoto, Japan). An antibody against 8-OHdG was from Nikken SEIL (Shizuoka, Japan). Wild-type mice (6–8 weeks old, ICR, male) were used. The experiments and procedures described here were carried out in accordance with the *Guide for the Care and Use of Laboratory Animals* as adopted and promulgated by the National Institutes of Health (Institute of Laboratory Animal Resources, 1996) and were approved by the Animal Care Committee of Kumamoto University.

Treatment of Mice with PPE, CS, and PC-SOD. Mice maintained under anesthesia with chloral hydrate (500 mg/kg) were given one intratracheal injection of PPE (50 or 100 μg/mouse) in phosphate-buffered saline (30 μl/mouse) by use of a micropipette (p200) to induce pulmonary emphysema. Commercial (nonfiltered) cigarettes (Peace; Japan Tobacco Inc., Tokyo, Japan) that yielded 28 mg of tar and 2.3 mg of nicotine on a standard smoking regimen were used. For exposure of mice to CS, 15 to 20 mice were placed in a chamber (volume, 45 L). Mice were exposed to the smoke of two cigarettes for 25 min, three times a day for 3 days. In the chronic model, mice were exposed to the smoke of one cigarette for 35 min, three times a day, 5 days a week, for 4 weeks. Each cigarette was puffed 15 times for 5 min.

For intravenous administration of PC-SOD, PC-SOD was dissolved in 5% xylitol and administered via the tail vein. For control mice, 5% xylitol solution was administered. The first administration of PC-SOD was performed just before PPE administration.

For the administration of PC-SOD by inhalation, five to seven mice were placed in a chamber (volume, 45 L). PC-SOD was dissolved in 10 ml of 5% xylitol, and an ultrasonic nebulizer (NE-U17 from Omron, Tokyo, Japan) that was connected to the chamber was used to nebulize the entire volume of the PC-SOD solution in 30 min. For control mice, 5% xylitol solution was subjected to nebulization. Mice were kept in the chamber for another 10 min after the 30 min of nebulization. The first inhalation of PC-SOD was performed just before PPE administration.

The amount of α1-antitrypsin in the plasma and proinflammatory mediators in BALF was measured by ELISA according to the manufacturer's protocol.

Preparation of BALF and Cell Count. BALF was collected by cannulating the trachea and lavaging the lung with 1 ml of sterile phosphate-buffered saline containing 50 units/ml heparin (two times). Approximately 1.8 ml of BALF was routinely recovered from each animal. The total cell number was counted using a hemocytometer. Cells were stained with Diff-Quik reagents after centrifugation with Cytospin 4, and the ratios of alveolar macrophages, lymphocytes, and neutrophils to total cells were determined.

Measurement of Production of Superoxide Anions. The production of superoxide anions was assayed by electron spin resonance (ESR) spin trapping with DPhPMPO as described previously (Karakawa et al., 2008). Cells collected from BALF were incubated with 0.9% NaCl containing 500 μM diethylenetriamine-*N*,*N*,*N*′,*N*″,*N*″-pentaacetic acid and 10 mM DPhPMPO for 10 min at 37°C. ESR

spectra were recorded at room temperature on a JES-TE200 ESR spectrometer (JEOL, Tokyo, Japan) under the following conditions: modulation frequency, 100 kHz; microwave frequency, 9.43 GHz; microwave power, 40 mW; scanning field, 335.2 ± 5 mT; sweep time, 2 min; field modulation width, 0.25 mT; receiver gain, 400; and time count, 0.3 s. Every buffer and solution used in the reaction mixture used for ESR measurement was treated with Chelex 100 resin (Bio-Rad Laboratories) before use to remove metals.

Histological and Immunohistochemical Analyses and Terminal Deoxynucleotidyl Transferase dUTP Nick-End Labeling Assay. Lung tissue samples were fixed for 24 h at a pressure of 25 cm H_2O, and then embedded in paraffin before being cut into 4 μm-thick sections.

For histological examination, sections were stained first with Mayer's hematoxylin and then with 1% eosin alcohol solution [hematoxylin and eosin (H and E) staining]. Samples were mounted with malinol and inspected with the aid of an Olympus (Tokyo, Japan) BX51 microscope. Twenty lines (500 μm) were drawn randomly on the image of sections stained with H and E, and the intersection points with the alveolar walls were counted to determine the mean linear intercept. The morphometric analysis at the light microscopic level was conducted by a blinded investigator.

For immunohistochemical analysis, sections were treated with 20 μg/ml protease K for antigen activation. Sections were blocked with 2.5% goat serum for 10 min, incubated for 12 h with an antibody against 8-OHdG (1:100 dilution) in the presence of 2.5% bovine serum albumin, and then incubated for 1 h with Alexa Fluor 488 goat anti-mouse IgG in the presence of DAPI (5 μg/ml). Samples were mounted with VECTASHIELD and inspected using fluorescence microscopy (Olympus BX51).

For the TUNEL assay, sections were incubated first with proteinase K (20 μg/ml) for 15 min at 37°C, then with TdTase and biotin 14-ATP for 1 h at 37°C, and finally with Alexa Fluor 488 conjugated with streptavidin and DAPI (5 μg/ml) for 2 h. Samples were mounted with VECTASHIELD and inspected with the aid of a fluorescence microscope (Olympus BX51).

Gelatin Zymography. The proteolytic activities of MMP-2 and MMP-9 were assessed by SDS-polyacrylamide gel electrophoresis using zymogram gels containing 0.1% gelatin as described previously (Namba et al., 2009). The protein concentration was determined by the Bradford method (Bradford, 1976). After electrophoresis at 4°C (10 μg of protein/lane), the gels were washed with 2.5% Triton X-100 for 30 min at room temperature and incubated with zymogram development buffer for 2 days at 37°C. Bands were visualized by staining with Coomassie brilliant blue.

Real-Time RT-PCR Analysis. Real-time RT-PCR was performed as described previously (Namba et al., 2009) with some modifications. Total RNA was extracted from pulmonary tissues using an RNeasy kit according to the manufacturer's protocol (QIAGEN). Samples (2.5 μg of RNA) were reverse-transcribed using a PrimeScript first-strand cDNA Synthesis Kit. Synthesized cDNA was used in real-time RT-PCR (Chromo 4 instrument; Bio-Rad Laboratories) experiments using iQ SYBR GREEN Supermix and analyzed with Opticon Monitor Software (Bio-Rad Laboratories). Specificity was confirmed by electrophoretic analysis of the reaction products and inclusion of template- or reverse transcriptase-free controls. To normalize the amount of total RNA present in each reaction, GAPDH cDNA was used as an internal standard.

Primers were designed using the Primer3 website (http://frodo.wi.mit.edu/primer3/). The primers used were (forward primer, reverse primer): TNF-α, 5′-cgtcagccgatttgctatct-3′, 5′-cggactccgcaaagtctaag-3′; IL-1β, 5′-gatcccaagcaatacccaaa-3′, 5′-ggggaactctgcagactcaa-3′; IL-6, 5′-ctggagtcacagaaggagtgg-3′, 5′-ggtttgccgagtagatctcaa-3′; MIP-2α, 5′-accctgccaagggttgacttc-3′, 5′-ggcacatcaggtacgatccag-3′; MCP-1, 5′-ctcacctgctgctactcattc-3′, 5′-gcttgaggtggttgtggaaaa-3′; KC, 5′-tgcacccaaaccgaagtcat-3′, 5′-ttgtcagaagccagcgttcac-3′; and GAPDH, 5′-aactttggcattgtggaagg-3′, 5′-acacattgggggtaggaaca-3′.

Analysis of Lung Function. Analysis of lung function was performed with a computer-controlled small-animal ventilator (FlexiVent; SCIREQ, Montreal, QC, Canada), as described previously (Kuraki et al., 2002). Mice were anesthetized with chloral hydrate (500 mg/kg), tracheotomized with an 8-mm section of metallic tubing, and mechanically ventilated at a rate of 150 breaths/min, using a tidal volume of 8.7 ml/kg and a positive end-expiratory pressure of 2 to 3 cm H_2O. The single-compartment model (snap shot) and the constant-phase model (forced oscillation technique) were applied to analyze lung function. Total respiratory system elastance and tissue elastance were measured by the snap shot and forced oscillation techniques, respectively. All data were analyzed using FlexiVent software (version 5.3) (SCIREQ).

Statistical Analysis. All values are expressed as the mean ± S.E.M. Two-way analysis of variance followed by the Tukey test or the Student's *t* test for unpaired results was used to evaluate differences between three or more groups or between two groups, respectively. Differences were considered to be significant for values of $P < 0.05$. We repeated the experiments at least two times as independent experiments (see figure legends) and selected one set of representative data to show in the figures. The stated number of test sample is not summation of independent plural experiments but is for only one independent experiment.

Results

Effect of PC-SOD on Elastase-Induced Pulmonary Emphysema. Pulmonary emphysema was induced in mice given a single (at day 0) intratracheal administration of PPE. The PPE-induced pulmonary inflammatory response can be monitored by determining the number of leukocytes (alveolar macrophages, lymphocytes, and neutrophils) in the BALF 3 days after the administration of PPE (50 μg/mouse). As shown in Fig. 1A, the total number of leukocytes and individual numbers of alveolar macrophages, lymphocytes, and neutrophils all were increased by the PPE treatment. This effect was suppressed by the simultaneous once-daily intravenous administration of PC-SOD, suggesting that PC-SOD ameliorates the PPE-induced inflammatory response. However, a higher dose of PC-SOD (30 kU/kg) did not suppress the PPE-induced inflammatory response (Fig. 1A), so in this study PC-SOD exhibited a bell-shaped dose-response profile, similar to that observed previously for intravenous administration of PC-SOD in animal models of other diseases (Ishihara et al., 2009; Tanaka et al., 2010). Intravenous administration of the higher dose (30 kU/kg) of PC-SOD alone (without PPE administration) did not affect the number of leukocytes in the BALF (data not shown).

PPE-induced pulmonary emphysema can be monitored by histopathological analysis and measurement of the mean linear intercept (an indicator of airspace enlargement caused by breakdown of the alveolar walls) 3 days after the administration of PPE. Histopathological analysis of pulmonary tissue using H and E staining revealed that PPE administration induced severe pulmonary damage (infiltration of leukocytes and breakdown of the alveolar walls) and these phenomena were suppressed by the intravenous administration of low doses (1.5 and 3 kU/kg), but not of a high dose (30 kU/kg), of PC-SOD (Fig. 1B). The mean linear intercept was increased by the administration of PPE; this increase was suppressed by intravenous administration of low doses (1.5 and 3 kU/kg) of PC-SOD but was not significantly suppressed at the higher dose (30 kU/kg) (Fig. 1C). Pulmonary tissue damage and the increase in the mean linear intercept 14

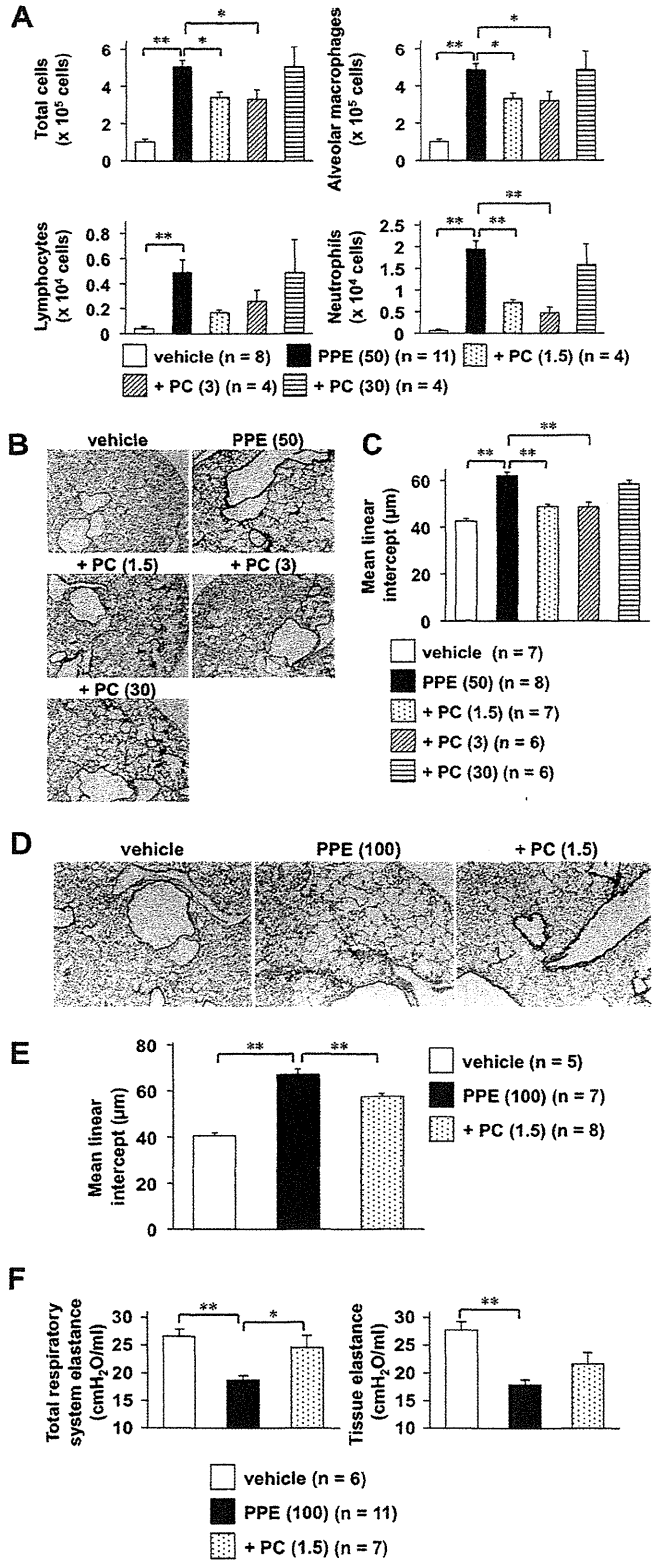

Fig. 1. Effect of intravenous administration of PC-SOD on PPE-induced pulmonary emphysema. Mice treated with (except vehicle) or without (vehicle) PPE (50 or 100 μg/mouse) once at day 0 were intravenously administered the indicated doses of PC-SOD (1.5, 3, or 30 kU/kg) once daily for 3 days (days 0–2) (A–C) or 14 days (days 0–13) (D–F). A, the total cell number and numbers of alveolar macrophages, lymphocytes, and neutrophils were determined at day 3 as described under *Materials and Methods*. B and D, sections of pulmonary tissue were prepared at days 3 or 14 and subjected to histopathological examination (H and E staining). C and E, airspace size was estimated by determining the mean linear intercept as described under *Materials and Methods*. F, at day 14, total respiratory system elastance and tissue elastance were determined as described under *Materials and Methods*. Values are mean ± S.E.M. *, $P < 0.05$; **, $P < 0.01$. Data are representative of two independent experiments.

days after PPE administration were also suppressed by the intravenous administration of PC-SOD (Fig. 1, D and E). We used higher dose of PPE (100 μg/mice) to monitor pulmonary emphysema 14 days after the administration of PPE.

The alteration in lung mechanics associated with pulmonary emphysema is characterized by a decrease in elastance (Kuraki et al., 2002). We thus examined the effect of intravenous administration of PC-SOD on PPE-induced alterations to lung mechanics, using a computer-controlled small-animal ventilator. Total respiratory system elastance (elastance of total lung including bronchi, bronchiole, and alveoli) and tissue elastance (elastance of alveoli) were reduced by PPE treatment, and intravenous administration of PC-SOD increased these indexes (Fig. 1F). These results suggest that not only PPE-induced pulmonary emphysema but also PPE-induced pulmonary dysfunction is ameliorated by intravenous administration of PC-SOD.

Effect of Inhalation of PC-SOD on Elastase-Induced Pulmonary Emphysema. We recently reported that inhalation of PC-SOD ameliorates bleomycin-induced pulmonary fibrosis (Tanaka et al., 2010). This route of administration does not show a bell-shaped dose-response profile (Tanaka et al., 2010) and may result in higher QOL for patients treated with PC-SOD. Thus, here we examined the effect of inhalation of PC-SOD on PPE-induced pulmonary emphysema. Mice were placed in a chamber connected to an ultrasonic nebulizer, thus exposing them to PC-SOD-containing vapor. We confirmed, by high-performance liquid chromatography analysis and measurement of SOD activity, that this treatment did not affect the structure and activity of the PC-SOD (data not shown). Inhalation of PC-SOD-containing vapor was repeated once daily for 3 or 14 days, and the mice were examined for PPE-induced pulmonary disorders. As shown in Fig. 2A, inhaled PC-SOD ameliorated the PPE-induced inflammatory response. This ameliorative effect was observed with not only low doses (30 and 60 kU/chamber) but also a high dose (600 kU/chamber) of PC-SOD, suggesting that the dose-response profile for this administration route is not bell-shaped. PPE-induced emphysematous lung damage and the increase in the mean linear intercept were also suppressed by inhalation of PC-SOD (Fig. 2, B–E), suggesting that inhalation of PC-SOD ameliorates PPE-induced pulmonary emphysema. Again, a bell-shaped dose-response profile was not observed for the ameliorative effect of inhalation of PC-SOD against PPE-induced pulmonary emphysema (Fig. 2, B and C). As shown in Table 1, inhalation of unmodified SOD (600 kU/chamber) did not affect the PPE-induced pulmonary inflammatory response and emphysema. This suggests that lecithinization of SOD potentiates its ameliorative effect against PPE-induced lung disorders, as is the case for dextran sulfate sodium-induced colitis and bleomycin-induced pulmonary fibrosis (Ishihara et al., 2009; Tanaka et al., 2010). We also found that inhalation of PC-SOD sup-

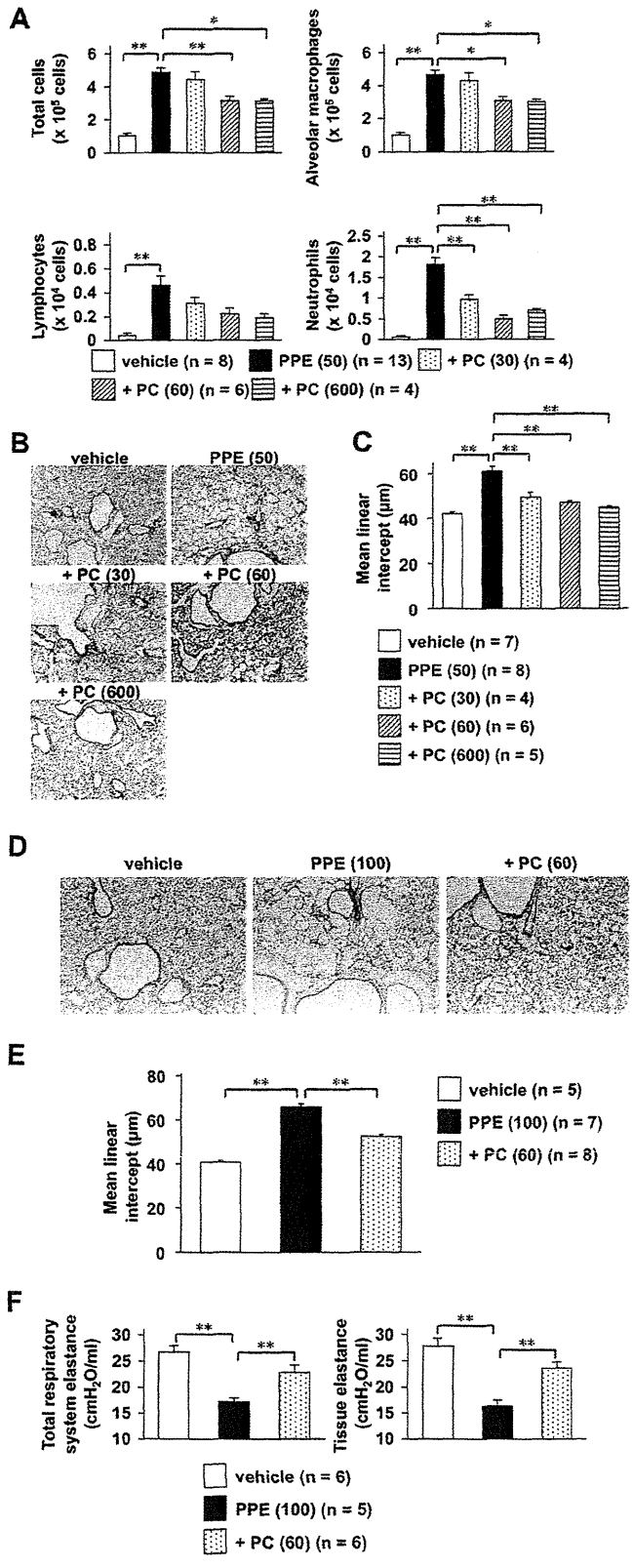

Fig. 2. Effect of inhalation of PC-SOD on PPE-induced pulmonary emphysema. Mice treated with (except vehicle) or without (vehicle) PPE (50 or 100 μg/mouse) once at day 0 inhaled the indicated doses of PC-SOD (30, 60, or 600 kU/chamber) once daily for 3 days (days 0–2) (A–C) or 14 days (days 0–13) (D–F). Inflammatory response (A), airspace size (B–E), and lung mechanics (F) were assessed as described in the legend of Fig. 1. Values are mean ± S.E.M. *, $P < 0.05$; **, $P < 0.01$. Data are representative of three independent experiments.

TABLE 1

Effect of inhalation of unmodified SOD on PPE-induced pulmonary emphysema

Mice were treated with a single dose of PPE (50 μg/mouse) at day 0 and inhaled unmodified SOD (U-SOD; 600 kU/chamber) once daily for 3 days (days 0–2). Inflammatory response and the mean linear intercept were assessed as described in the legend of Fig. 1. Values are mean ± S.E.M.

	PPE (50) (n = 8)	+ U-SOD (600 kU/chamber) (n = 4)
Total cells, $\times 10^5$	4.9 ± 0.33	4.9 ± 0.35
Alveolar macrophages, $\times 10^5$	4.7 ± 0.36	4.7 ± 0.33
Lymphocytes, $\times 10^4$	0.40 ± 0.07	0.35 ± 0.06
Neutrophils, $\times 10^4$	1.6 ± 0.15	1.3 ± 0.19
Mean linear intercept, μm	58.2 ± 1.30	57.7 ± 0.37

presses PPE-induced decreases in total respiratory system elastance and tissue elastance (Fig. 2F), suggesting that inhalation of PC-SOD ameliorates PPE-induced lung dysfunction. We confirmed that inhalation of PC-SOD alone did not induce pulmonary emphysema and dysfunction (Supplemental Fig. 1).

To consider the clinical relevance, it is important to examine the effect of the drug on predeveloped lesions in an animal model (Fig. 3). Thus, we examined the effect of inhalation of PC-SOD on predeveloped pulmonary emphysema. Once-daily inhalation of PC-SOD was started 3 days after the administration of PPE, and pulmonary emphysema and function were assessed at day 10. Inhalation of PC-SOD caused suppression of pulmonary emphysema at day 10, suggesting that the inhalation of PC-SOD is effective for predeveloped lesions.

The inhalation of PC-SOD also suppressed the PPE-induced alterations in lung mechanics at day 10 (Fig. 3C), suggesting that inhalation of PC-SOD suppresses the PPE-induced lung dysfunction, even when it is administered after the PPE.

Mechanism for the Ameliorative Effects of PC-SOD on PPE-Induced Pulmonary Emphysema. To confirm that inhaled PC-SOD decreases the pulmonary level of superoxide anion, we performed an immunohistochemical analysis to monitor the pulmonary level of 8-OHdG, the damaged nucleotide produced by various ROS, including the superoxide anion (Freeman et al., 2009). As shown in Fig. 4A, the pulmonary level of 8-OHdG was significantly increased by PPE administration, and this increase was clearly suppressed by inhalation of PC-SOD, suggesting that production of ROS in the lung was suppressed by inhalation of PC-SOD. We also used ESR analysis to monitor the production of superoxide anion in cells in BALF. The ESR spectrum was consistent with a previously reported DPhPMPO-OOH spectrum (a hyperfine coupling constant of a^N = 1.24 mT, a^H_β = 1.16 mT, a^P = 3.95 mT) (Karakawa et al., 2008). As shown in Fig. 4, B and C, the peak of a radical spin adduct of the ESR spectrum corresponding to the amount of superoxide anion (DPhPMPO-OOH adduct) was higher for cells prepared from PPE-administered mice than for cells from control mice. Inhalation of PC-SOD lowered this peak, suggesting that inhaled PC-SOD suppresses PPE-induced production of superoxide anions in the lung.

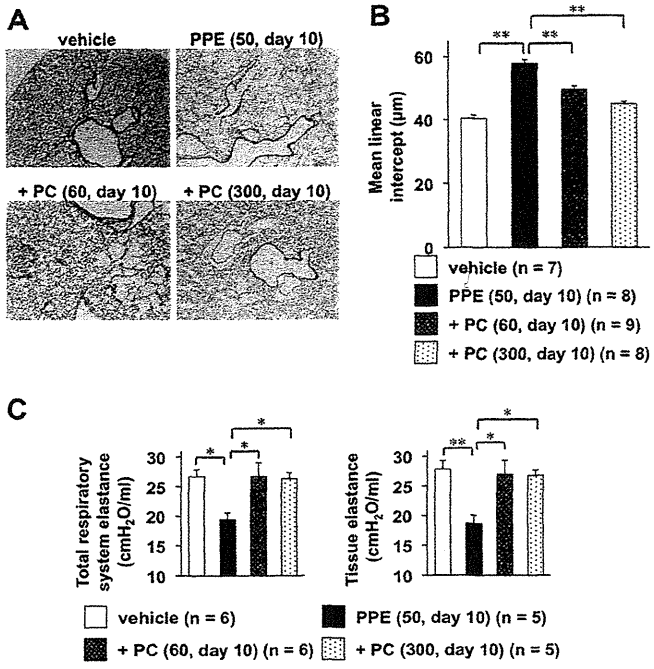

Fig. 3. Effect of PC-SOD on predeveloped pulmonary emphysema. Mice treated with (except vehicle) or without (vehicle) PPE (50 μg/mouse) once at day 0 inhaled the indicated doses of PC-SOD (kU/chamber) once daily from days 3 to 9. Airspace size (A and B) and lung mechanics (C) were assessed at day 10 as described in the legend of Fig. 1. Values are mean ± S.E.M. *, $P < 0.05$; **, $P < 0.01$. Data are representative of two independent experiments.

As described in Introduction, pulmonary cell apoptosis plays an important role in the pathogenesis of COPD and PPE-induced pulmonary emphysema. We examined the effect of inhalation of PC-SOD on PPE-induced pulmonary cell death by using the TUNEL assay. TUNEL-positive cells (indicative of cell death) increased in response to administration of PPE, and this increase was suppressed by simultaneous inhalation of PC-SOD (Fig. 4, D and E), suggesting that PC-SOD protects pulmonary cells from PPE-induced cell death, and this effect is involved in the ameliorative effects of inhalation of PC-SOD against PPE-induced pulmonary emphysema.

To examine the effect of inhalation of PC-SOD on the PPE-dependent imbalance in proteases and antiproteases, we first examined the activity of MMPs, MMP-2 and MMP-9, using gelatin zymography. The band intensities of MMP-2 and MMP-9, indicative of MMP-2 and MMP-9 activities, were higher for lung tissues prepared from PPE-administered mice than for those from control mice, and this increase was suppressed in mice that had inhaled PC-SOD (Fig. 5, A and B). We also examined the serum level of α1-antitrypsin by ELISA and found that the level of α1-antitrypsin was decreased by PPE administration and partially recovered by simultaneous inhalation of PC-SOD (Fig. 5C). These results suggest that inhalation of PC-SOD improves the PPE-dependent protease/antiprotease imbalance and this effect is involved in the ameliorative effects of inhalation of PC-SOD against PPE-induced pulmonary emphysema.

We also examined the effect of inhalation of PC-SOD on the mRNA expression of proinflammatory cytokines (TNF-α, IL-1β, and IL-6) and chemokines (MIP-2, MCP-1, and KC) in

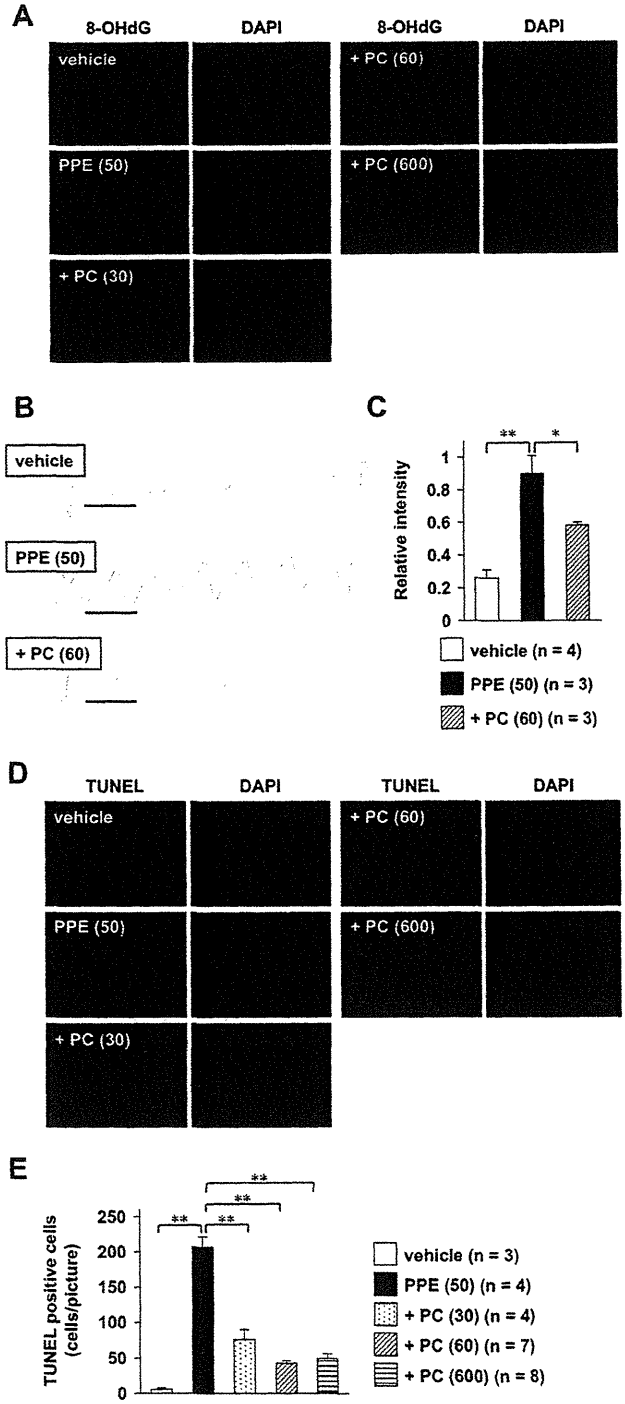

Fig. 4. Effect of PC-SOD on the PPE-induced increase in the level of 8-OHdG, production of superoxide anions, and pulmonary cell death. Mice treated with PPE inhaled PC-SOD (kU/chamber) for 3 days (days 0–2) (A, D, and E) or 1 day (day 0) (B and C) as described in the legend of Fig. 2. A, D, and E, sections of pulmonary tissue were prepared at day 3. A, sections were subjected to immunohistochemical analysis with an antibody against 8-OHdG or DAPI staining. B, cells in BALF were collected at day 1, incubated with a spin trap agent (DPhPMPO), and subjected to radical adduct ESR spectrum analysis to determine the amount of superoxide anion present. C, the intensity of the ESR signal of the superoxide anion adduct (DPhPMPO–OOH adduct shown by the bar in B) was determined. D, sections were subjected to TUNEL assay or DAPI staining. E, the number of TUNEL-positive cells was counted. Values are mean ± S.E.M. *, $P < 0.05$; **, $P < 0.01$. Data are representative of two independent experiments.

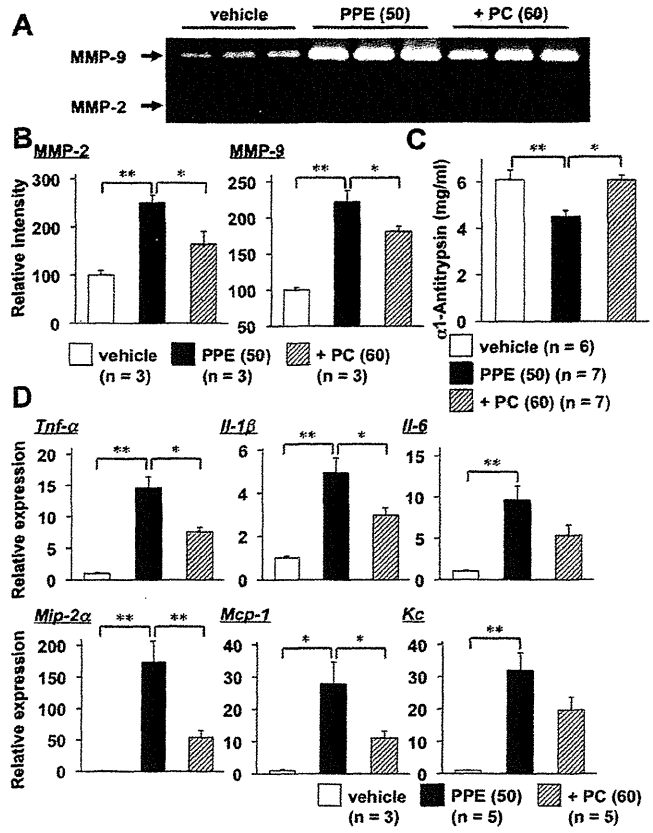

Fig. 5. Effect of PC-SOD on PPE-induced MMP activation, decrease in the serum level of α1-antitrypsin, and alteration in gene expression. Mice treated with PPE inhaled PC-SOD (kU/chamber) for 3 days (days 0–2) (A and B) or for 1 day (day 0) (C and D) as described in the legend of Fig. 2. A, pulmonary tissues were obtained at day 3, and MMP-2 and MMP-9 activities were measured as described under *Materials and Methods* . B, the intensity of the bands corresponding to the latent forms of MMP-2 and MMP-9 was determined and expressed relative to the control samples (vehicle). C, the serum level of α1-antitrypsin was determined by ELISA at day 1. Total RNA was extracted and subjected to real-time RT-PCR using a specific primer for each gene. D, values normalized to the *gapdh* gene are expressed relative to the control samples (vehicle). Values are mean ± S.E.M. *, $P < 0.05$; **, $P < 0.01$. Data are representative of two independent experiments.

lung tissues. The mRNA expression of all of these proinflammatory cytokines and chemokines was induced by PPE administration, and in most cases this induction was suppressed by inhalation of PC-SOD. We also measured the amounts of these proinflammatory cytokines and chemokines in BALF by ELISA and confirmed the data of mRNA expression (Supplemental Fig. 2). These results suggest that inhalation of PC-SOD suppresses PPE-induced expression of proinflammatory cytokines and chemokines in the lung and this effect is involved in the ameliorative effects of PC-SOD inhalation on the PPE-induced pulmonary inflammatory response and resulting emphysema.

Effect of PC-SOD on CS-Induced Inflammatory Response. PPE-induced pulmonary emphysema is a convenient and reproducible model of COPD; thus, this model has been used frequently for the evaluation of drugs for COPD. However, it is believed that the CS-induced pulmonary emphysema model is more relevant as an animal model of COPD, because it induces the disease using the same stimulus rather than just replicating one of the mechanisms of the disease. Thus, we examined the effect of PC-SOD on CS-induced pulmonary emphysema. Mice were assessed for a pulmonary inflammatory response at 3 days after exposure to CS. We found that this treatment induced an inflammatory response, as was the case for treatment with elastase (Fig. 6A). As shown in Fig. 6A, intravenously administered PC-SOD ameliorated the CS-induced increase in the total number of leukocytes and individual numbers of alveolar macrophages, lymphocytes, and neutrophils in the BALF, suggesting that intravenous administration of PC-SOD ameliorates CS-induced pulmonary inflammation. As shown in Fig. 6B, inhalation of PC-SOD also ameliorated the CS-induced inflammatory response.

We also examined the effect of PC-SOD on CS-induced pulmonary emphysema and dysfunction. Exposure of mice to CS for 4 weeks caused emphysematous lung damage and the increase in the mean linear intercept and this emphysema was suppressed by simultaneous inhalation of PC-SOD (Supplemental Fig. 3, A and B). We also found that exposure of mice to CS for 4 weeks caused decreases in total respiratory system elastance and tissue elastance, and this decrease was suppressed by simultaneous inhalation of PC-SOD (Supplemental Fig. 3C). These results suggest that inhalation of PC-SOD is effective for the treatment of CS-related pulmonary inflammation, emphysema, and lung dysfunction, including COPD.

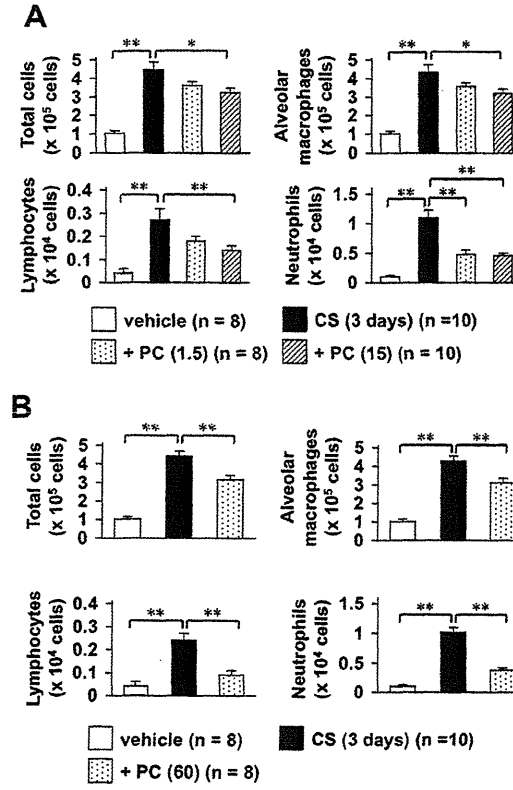

Fig. 6. Effect of PC-SOD on CS-induced inflammatory response. Mice were exposed to CS for 3 days as described under *Materials and Methods*. Mice were also intravenously administered PC-SOD (kU/kg) (A) or inhaled with PC-SOD (kU/chamber) (B) as described in the legends of Figs. 1 and 2. Inflammatory response was assessed as described in the legend of Fig. 1. Values are mean ± S.E.M. *, $P < 0.05$; **, $P < 0.01$. Data are representative of two independent experiments.

Discussion

In this study, we used PC-SOD, a derivative of SOD with higher stability in plasma and a higher affinity for tissue, which shows greater therapeutic effects than SOD in animal models of various inflammatory diseases, such as IPF, colitis, focal cerebral ischemic injury, and spinal cord injury-induced motor dysfunction (Hori et al., 1997; Tamagawa et al., 2000; Ishihara et al., 2009; Tanaka et al., 2010). We have clearly shown that PC-SOD ameliorates pulmonary emphysema. This result indicates the therapeutic potential of SOD against COPD-related pulmonary emphysema and is consistent with previous results that show transgenic mice expressing SOD bear a phenotype of resistance to pulmonary emphysema (Foronjy et al., 2006; Petrache et al., 2008). In a phase I clinical study, intravenously administered PC-SOD (40–160 mg) had a terminal half-life of more than 24 h with good safety and tolerability (Broeyer et al., 2008; Suzuki et al., 2008a). Published results of a phase II clinical study have shown that intravenously administered PC-SOD (40 or 80 mg) significantly improves the symptoms of ulcerative colitis patients, which involves ROS (Suzuki et al., 2008b). A phase II clinical study has shown that intravenously administered PC-SOD (40 or 80 mg) is therapeutically effective against IPF as judged by monitoring the serum level of marker proteins (lactate dehydrogenase and surfactant protein-A). Because the safety and efficacy of PC-SOD were shown in not only the animal model but also in clinical studies the application of PC-SOD for COPD is realistic.

Here, we have shown that not only intravenous administration but also inhalation of PC-SOD ameliorates pulmonary emphysema. We believe that inhalation is a clinically more valuable route of administration than the intravenous route for two reasons. First, PC-SOD administered by inhalation does not have a bell-shaped dose-response profile. Bell-shaped dose-response curves are of clinical concern because they may reflect the presence of side effects. The lack of a bell-shaped dose-response profile upon inhalation has also been observed for bleomycin-induced pulmonary fibrosis (Tanaka et al., 2010). Because the efficacy of intravenous administration of higher doses of PC-SOD on bleomycin-induced pulmonary fibrosis was restored by simultaneous administration of catalase, which converts hydrogen peroxide to water and oxygen, the ineffectiveness of high doses of PC-SOD is probably caused by the accumulation of hydrogen peroxide (Tanaka et al., 2010). However, the reason inhalation of PC-SOD does not show the bell-shaped dose-response profile remains unknown. Second, patients treated with PC-SOD administered by inhalation would have a higher QOL than those treated intravenously. Although a phase II clinical study has shown that intravenously administered PC-SOD (40 or 80 mg) is effective for both ulcerative colitis (Suzuki et al., 2008b) and IPF, the main obstacle against proceeding into the next stage of clinical study is the poor QOL for patients undergoing the current clinical protocol of PC-SOD administration (daily intravenous infusion for 4 weeks). Furthermore, in a phase II clinical study for IPF, the plasma levels of markers (lactate dehydrogenase and surfactant protein A) but not forced vital capacity were modified by intravenous administration of PC-SOD, suggesting that a longer period of treatment with PC-SOD is required to improve forced vital capacity in patients with IPF. However, daily intravenous infusion for a longer period is not practical. Therefore, we propose that inhalation of PC-SOD for a longer period may be effective not only for IPF but also for COPD and would maintain the QOL of patients. The therapeutic potential of inhalation of PC-SOD for the treatment of COPD is also supported by observations made in this study: inhalation of PC-SOD ameliorated not only PPE-induced pathological alterations but also PPE-induced functional changes, and inhalation of PC-SOD was effective even for predeveloped pulmonary emphysema (stimulation of spontaneous restoration from pulmonary emphysema and suppression of progression of pulmonary dysfunction). Drugs for COPD should suppress both the inflammatory response and emphysematous lung destruction. Because ROS, especially superoxide anions, are suggested to induce both an inflammatory response and emphysematous lung destruction (Mak, 2008), PC-SOD was predicted to suppress both of these events. In fact, we showed that inhalation of PC-SOD suppresses a PPE-induced increase in leukocytes in BALF and the expression of proinflammatory cytokines and chemokines. We also showed that inhalation of PC-SOD suppresses PPE-induced emphysematous lung destruction. Both apoptosis and protease/antiprotease imbalance seem to be involved in emphysematous lung destruction associated with COPD (Demedts et al., 2006; Rabe et al., 2007; Petrache et al., 2008). We have shown that inhalation of PC-SOD suppresses PPE-induced pulmonary cell death and protease/antiprotease imbalance (activation of MMPs and decrease in the level of α1-antitrypsin). We recently reported that PC-SOD protects cultured lung epithelial cells from menadione (a superoxide anion-releasing drug)-induced cell death (Tanaka et al., 2010). It has also been reported that oxidative molecules activate MMPs and suppress the expression of α1-antitrypsin (Desrochers and Weiss, 1988; Greenlee et al., 2007; Mak, 2008; Wan et al., 2008). Thus, it seems that a PC-SOD-dependent decrease in the level of superoxide anions is responsible for the inhibitory effect of PC-SOD on PPE-induced pulmonary cell death and the protease/antiprotease imbalance.

One of the current standard clinical protocols for treatment of patients with COPD is administration of a long-acting β_2-agonist or anticholinergic along with corticosteroid inhalation. This combination regime reduces the annual rate of exacerbation and improves health status and spirometric values, although it does not improve the mortality rate with statistical significance (Calverley et al., 2007). β_2-Agonists and anticholinergics are effective in improving the airflow limitation associated with COPD (Rabe et al., 2007). On the other hand, some reports have suggested that treatment with corticosteroids does not clearly modulate the inflammatory response in patients with COPD or in a CS-induced pulmonary emphysema animal model (Rabe et al., 2007; Fox and Fitzgerald, 2009). Based on these previous observations and those in this study that inhalation of PC-SOD is effective against the CS-induced inflammatory response, we consider that a combination regime of administration of a long-acting β_2-agonist (or anticholinergics) along with inhalation of PC-SOD, instead of corticosteroids, may be therapeutically beneficial for patients with COPD.

Authorship Contributions

Participated in research design: K.-I. Tanaka and Mizushima.
Conducted experiments: K.-I. Tanaka, Y. Tanaka, and Miyazaki.

Contributed new reagents or analytic tools: Namba, Sato, and Aoshiba.

Performed data analysis: K.-I. Tanaka and Sato.

Wrote or contributed to the writing of the manuscript: K.-I. Tanaka, Aoshiba, Azuma, and Mizushima.

References

Barnes PJ and Stockley RA (2005) COPD: current therapeutic interventions and future approaches. *Eur Respir J* **25:**1084–1106.

Bradford MM (1976) A rapid and sensitive method for the quantitation of microgram quantities of protein utilizing the principle of protein-dye binding. *Anal Biochem* **72:**248–254.

Broeyer FJ, van Aken BE, Suzuki J, Kemme MJ, Schoemaker HC, Cohen AF, Mizushima Y, and Burggraaf J (2008) The pharmacokinetics and effects of a long-acting preparation of superoxide dismutase (PC-SOD) in man. *Br J Clin Pharmacol* **65:**22–29.

Calverley PM, Anderson JA, Celli B, Ferguson GT, Jenkins C, Jones PW, Yates JC, Vestbo J, and TORCH Investigators (2007) Salmeterol and fluticasone propionate and survival in chronic obstructive pulmonary disease. *N Engl J Med* **356:**775–789.

Daga MK, Chhabra R, Sharma B, and Mishra TK (2003) Effects of exogenous vitamin E supplementation on the levels of oxidants and antioxidants in chronic obstructive pulmonary disease. *J Biosci* **28:**7–11.

Demedts IK, Demoor T, Bracke KR, Joos GF, and Brusselle GG (2006) Role of apoptosis in the pathogenesis of COPD and pulmonary emphysema. *Respir Res* **7:**53.

Desrochers PE and Weiss SJ (1988) Proteolytic inactivation of α-1-proteinase inhibitor by a neutrophil metalloproteinase. *J Clin Invest* **81:**1646–1650.

Foronjy RF, Mirochnitchenko O, Propokenko O, Lemaitre V, Jia Y, Inouye M, Okada Y, and D'Armiento JM (2006) Superoxide dismutase expression attenuates cigarette smoke- or elastase-generated emphysema in mice. *Am J Respir Crit Care Med* **173:**623–631.

Fox JC and Fitzgerald MF (2009) The role of animal models in the pharmacological evaluation of emerging anti-inflammatory agents for the treatment of COPD. *Curr Opin Pharmacol* **9:**231–242.

Freeman TA, Parvizi J, Della Valle CJ, and Steinbeck MJ (2009) Reactive oxygen and nitrogen species induce protein and DNA modifications driving arthrofibrosis following total knee arthroplasty. *Fibrogenesis Tissue Repair* **2:**5.

Greenlee KJ, Werb Z, and Kheradmand F (2007) Matrix metalloproteinases in lung: multiple, multifarious, and multifaceted. *Physiol Rev* **87:**69–98.

Hori Y, Hoshino J, Yamazaki C, Sekiguchi T, Miyauchi S, Mizuno S, and Horie K (1997) Effect of lecithinized-superoxide dismutase on the rat colitis model induced by dextran sulfate sodium. *Jpn J Pharmacol* **74:**99–103.

Igarashi R, Hoshino J, Ochiai A, Morizawa Y, and Mizushima Y (1994) Lecithinized superoxide dismutase enhances its pharmacologic potency by increasing its cell membrane affinity. *J Pharmacol Exp Ther* **271:**1672–1677.

Igarashi R, Hoshino J, Takenaga M, Kawai S, Morizawa Y, Yasuda A, Otani M, and Mizushima Y (1992) Lecithinization of superoxide dismutase potentiates its protective effect against Forssman antiserum-induced elevation in guinea pig airway resistance. *J Pharmacol Exp Ther* **262:**1214–1219.

Institute of Laboratory Animal Resources (1996) *Guide for the Care and Use of Laboratory Animals*, 7th ed. Institute of Laboratory Animal Resources, Commission on Life Sciences, National Research Council, Washington DC.

Ishihara T, Tanaka K, Tasaka Y, Namba T, Suzuki J, Ishihara T, Okamoto S, Hibi T, Takenaga M, Igarashi R, et al. (2009) Therapeutic effect of lecithinized superoxide dismutase against colitis. *J Pharmacol Exp Ther* **328:**152–164.

Karakawa T, Sato K, Muramoto Y, Mitani Y, Kitamado M, Iwanaga T, Nabeshima T, Maruyama K, Nakagawa K, Ishida K, et al. (2008) Applicability of new spin trap agent, 2-diphenylphosphinoyl-2-methyl-3,4-dihydro-2*H*-pyrrole *N*-oxide, in biological system. *Biochem Biophys Res Commun* **370:**93–97.

Kinnula VL and Crapo JD (2003) Superoxide dismutases in the lung and human lung diseases. *Am J Respir Crit Care Med* **167:**1600–1619.

Kondo T, Tagami S, Yoshioka A, Nishimura M, and Kawakami Y (1994) Current smoking of elderly men reduces antioxidants in alveolar macrophages. *Am J Respir Crit Care Med* **149:**178–182.

Kuraki T, Ishibashi M, Takayama M, Shiraishi M, and Yoshida M (2002) A novel oral neutrophil elastase inhibitor (ONO-6818) inhibits human neutrophil elastase-induced emphysema in rats. *Am J Respir Crit Care Med* **166:**496–500.

Mak JC (2008) Pathogenesis of COPD. Part II. Oxidative-antioxidative imbalance. *Int J Tuberc Lung Dis* **12:**368–374.

Miravitlles M and Anzueto A (2009) Insights into interventions in managing COPD patients: lessons from the TORCH and UPLIFT studies. *Int J Chron Obstruct Pulmon Dis* **4:**185–201.

Nadeem A, Raj HG, and Chhabra SK (2005) Increased oxidative stress and altered levels of antioxidants in chronic obstructive pulmonary disease. *Inflammation* **29:**23–32.

Namba T, Homan T, Nishimura T, Mima S, Hoshino T, and Mizushima T (2009) Up-regulation of S100P expression by non-steroidal anti-inflammatory drugs and its role in anti-tumorigenic effects. *J Biol Chem* **284:**4158–4167.

Owen CA (2005) Proteinases and oxidants as targets in the treatment of chronic obstructive pulmonary disease. *Proc Am Thorac Soc* **2:**373–385; discussion 394–395.

Peto R, Chen ZM, and Boreham J (1999) Tobacco–the growing epidemic. *Nat Med* **5:**15–17.

Petrache I, Medler TR, Richter AT, Kamocki K, Chukwueke U, Zhen L, Gu Y, Adamowicz J, Schweitzer KS, Hubbard WC, et al. (2008) Superoxide dismutase protects against apoptosis and alveolar enlargement induced by ceramide. *Am J Physiol Lung Cell Mol Physiol* **295:**L44–L53.

Pinamonti S, Leis M, Barbieri A, Leoni D, Muzzoli M, Sostero S, Chicca MC, Carrieri A, Ravenna F, Fabbri LM, et al. (1998) Detection of xanthine oxidase activity products by EPR and HPLC in bronchoalveolar lavage fluid from patients with chronic obstructive pulmonary disease. *Free Radic Biol Med* **25:**771–779.

Rabe KF, Hurd S, Anzueto A, Barnes PJ, Buist SA, Calverley P, Fukuchi Y, Jenkins C, Rodriguez-Roisin R, van Weel C, et al. (2007) Global strategy for the diagnosis, management, and prevention of chronic obstructive pulmonary disease: GOLD executive summary. *Am J Respir Crit Care Med* **176:**532–555.

Rahman I and Adcock IM (2006) Oxidative stress and redox regulation of lung inflammation in COPD. *Eur Respir J* **28:**219–242.

Suzuki J, Broeyer F, Cohen A, Takebe M, Burggraaf J, and Mizushima Y (2008a) Pharmacokinetics of PC-SOD, a lecithinized recombinant superoxide dismutase, after single- and multiple-dose administration to healthy Japanese and Caucasian volunteers. *J Clin Pharmacol* **48:**184–192.

Suzuki Y, Matsumoto T, Okamoto S, and Hibi T (2008b) A lecithinized superoxide dismutase (PC-SOD) improves ulcerative colitis. *Colorectal Dis* **10:**931–934.

Tamagawa K, Taooka Y, Maeda A, Hiyama K, Ishioka S, and Yamakido M (2000) Inhibitory effects of a lecithinized superoxide dismutase on bleomycin-induced pulmonary fibrosis in mice. *Am J Respir Crit Care Med* **161:**1279–1284.

Tanaka K, Ishihara T, Azuma A, Kudoh S, Ebina M, Nukiwa T, Sugiyama Y, Tasaka Y, Namba T, Ishihara T, et al. (2010) Therapeutic effect of lecithinized superoxide dismutase on bleomycin-induced pulmonary fibrosis. *Am J Physiol Lung Cell Mol Physiol* **298:**L348–L360.

Valenca SS, Bezerra FS, Romana-Souza B, Paiva RO, Costa AM, and Porto LC (2008) Supplementation with vitamins C and E improves mouse lung repair. *J Nutr Biochem* **19:**604–611.

Valentin F, Bueb JL, Kieffer P, Tschirhart E, and Atkinson J (2005) Oxidative stress activates MMP-2 in cultured human coronary smooth muscle cells. *Fundam Clin Pharmacol* **19:**661–667.

Wan R, Mo Y, Zhang X, Chien S, Tollerud DJ, and Zhang Q (2008) Matrix metalloproteinase-2 and -9 are induced differently by metal nanoparticles in human monocytes: The role of oxidative stress and protein tyrosine kinase activation. *Toxicol Appl Pharmacol* **233:**276–285.

Yao H, Arunachalam G, Hwang JW, Chung S, Sundar IK, Kinnula VL, Crapo JD, and Rahman I (2010) Extracellular superoxide dismutase protects against pulmonary emphysema by attenuating oxidative fragmentation of ECM. *Proc Natl Acad Sci USA* **107:**15571–15576.

Address correspondence to: Dr. Tohru Mizushima, Graduated School of Medical and Pharmaceutical Sciences, Kumamoto University, 5-1 Oe-honmachi, Kumamoto 862-0973, Japan. E-mail: mizu@gpo.kumamoto-u.ac.jp

Biochemical Pharmacology 82 (2011) 728–736

Contents lists available at ScienceDirect

Biochemical Pharmacology

journal homepage: www.elsevier.com/locate/biochempharm

Stimulation of gastric ulcer healing by heat shock protein 70

Tomoaki Ishihara, Shintaro Suemasu, Teita Asano, Ken-ichiro Tanaka, Tohru Mizushima *

Department of Analytical Chemistry, Faculty of Pharmacy, Keio University, 1-5-30, Shibakoen, Minato-ku, Tokyo 105-8512, Japan

ARTICLE INFO

Article history:
Received 31 May 2011
Accepted 21 June 2011
Available online 28 June 2011

Keywords:
Ulcer healing
Heat shock protein 70
Geranylgeranylacetone
Proliferation
Angiogenesis

ABSTRACT

It is important in treatment of gastric ulcers to not only prevent further ulcer formation but also enhance ulcer healing. When cells are exposed to gastric irritants, expression of heat shock proteins (HSPs) is induced, making the cells resistant to the irritants. We recently reported direct evidence that HSPs, especially HSP70, are preventive against irritant-induced gastric ulcer formation. Gastric ulcer healing is a process involving cell proliferation and migration at the gastric ulcer margin and angiogenesis in granulation tissue. In this study, we have examined the role of HSP70 in gastric ulcer healing. Gastric ulcers were produced by focal and serosal application of acetic acid. Expression of HSP70 was induced in both the gastric ulcer margin and granulation tissue. Compared with wild-type mice, gastric ulcer healing was accelerated in transgenic mice expressing HSP70, and both cell proliferation at the gastric ulcer margin and angiogenesis in granulation tissue were enhanced. Oral administration of geranylgeranylacetone, an inducer of HSPs, to wild-type mice, either prior to or after ulcer formation, not only induced expression of HSP70 in the stomach but also accelerated gastric ulcer healing. On the other hand, oral administration of purified recombinant HSP70 prior to the ulcer formation, but not after formation, stimulated gastric ulcer healing. This study provides the first evidence that HSP70 accelerates gastric ulcer healing. The results also suggest that both the HSP70 produced prior to ulcer formation and released from damaged cells, and the HSP70 produced after ulcer formation are involved in this accelerated healing process.

1. Introduction

The balance between aggressive and defensive factors determines the development of gastric lesions, with either a relative increase in aggressive factors or a relative decrease in defensive factors resulting in lesions. The gastric mucosa is challenged by a variety of both endogenous and exogenous irritants (aggressive factors), including ethanol, gastric acid, pepsin, reactive oxygen species, non-steroidal anti-inflammatory drugs (NSAIDs) and *Helicobacter pylori* [1]. In order to protect the gastric mucosa, a complex defence system, which includes the production of surface mucus (gastric mucin) and bicarbonate and the regulation of gastric mucosal blood flow has evolved. Prostaglandins (PGs), in particular PGE_2, enhance these protective mechanisms, and are therefore thought to be major gastric defensive factors [2].

Recently, heat shock proteins (HSPs) have also attracted considerable attention as major gastric defensive factors. When cells are exposed to stressors, HSPs are induced in a manner that is dependent on a transcription factor, heat shock factor 1 (HSF1). The up-regulation of HSPs, especially that of HSP70, provides resistance to such stressors given that intracellular HSPs re-fold or degrade denatured proteins produced by the stressors [3,4]. We recently reported that HSF1-null mice or transgenic mice expressing HSP70 show sensitive or resistant phenotypes, respectively, to irritant-induced gastric lesions [5,6], providing genetic evidence that HSPs, especially HSP70, play important roles in the protection of gastric mucosa from irritant-induced lesion formation. Interestingly, geranylgeranylacetone (GGA), one of the standard anti-ulcer drugs on the Japanese market, has been reported to be an HSP-inducer, up-regulating HSPs not only in cultured gastric mucosal cells but also at the gastric mucosa [7–10]. We recently showed that the HSP-inducing activity of GGA mainly contributes to its gastro-protective activity against ethanol and NSAIDs [5,6]. In these experiments, we used 50–200 mg/kg doses of GGA by oral administration 1 h before the administration of ethanol or NSAIDs and observed the ulcer formation 4 h or 8 h after the administration of ethanol or NSAIDs, respectively [5,6].

Abbreviations: NSAIDs, non-steroidal anti-inflammatory drugs; PGs, prostaglandins; HSPs, heat shock proteins; HSF1, heat shock factor 1; GGA, geranylgeranylacetone; bFGF, basic fibroblast growth factor; IGF, insulin-like growth factor; TGF, transforming growth factor; VEGF, vascular endothelial growth factor; BrdU, 5-bromo-2′-deoxyuridine; EIA, enzyme immuno assay; ELISA, enzyme-linked immunosorbent assay; GAPDH, glyceraldehyde-3-phosphate dehydrogenase; DAMP, damage-associated molecular patterns.

* Corresponding author. Tel.: +81 3 5400 2628; fax: +81 3 5400 2628.
E-mail addresses: mizushima-th@pha.keio.ac.jp, mizu@gpo.kumamoto-u.ac.jp (T. Mizushima).

0006-2952/$ – see front matter © 2011 Elsevier Inc. All rights reserved.
doi:10.1016/j.bcp.2011.06.030

HSP70 has also been detected in extracellular compartments and the actions of extracellular HSP70 have recently been paid much attention. It has been reported that HSP70 could be released from cells through both passive (leaked from necrotic cells) and active (released by exocytosis) routes [11,12]. Such extracellular HSP70 binds to high-affinity receptors, including toll-like receptors, to induce the innate immune response [13–16]. Although extracellular HSP70 should be present at the gastric mucosa, especially when ulcerated, the role of extracellular HSP70 at this site is unknown.

Gastric ulcer healing is a complex process that includes inflammatory response (such as an increase in the level of PGE_2), re-epithelialization due to cell proliferation and migration at the gastric ulcer margin and angiogenesis in granulation tissue [17–20]. Expression of growth factors such as basic fibroblast growth factor (bFGF), insulin-like growth factor (IGF), transforming growth factor (TGF)-β1 and vascular endothelial growth factor (VEGF) is induced by inflammatory responses and they activate epithelial cell migration and proliferation at the gastric ulcer margin and angiogenesis in granulation tissue to enhance ulcer healing [17,21–23].

For the effective treatment of gastric ulcers, not only the prevention of further ulcer formation, but also the enhancement of ulcer healing is important. However, no data have been reported for the role of HSP70 in gastric ulcer healing. In this study, we have examined the role of HSP70 in gastric ulcer healing, using transgenic mice expressing HSP70 and in response to treatment with GGA. The results suggest that expression of HSP70 accelerates gastric ulcer healing by increasing the level of PGE_2 and the expression of growth factors, thereby stimulating cell proliferation at the gastric ulcer margin and angiogenesis in granulation tissue. The results also suggest that both intracellular and extracellular HSP70 are involved in this acceleration.

2. Materials and methods

2.1. Chemicals and animals

GGA was a gift from Eisai (Tokyo, Japan). Formaldehyde, bovine serum albumin (BSA) and 5-bromo-2′-deoxyuridine (BrdU) were obtained from Sigma (St. Louis, MO). A PGE_2 enzyme immuno assay (EIA) kit was purchased from Cayman Chemical (Ann Arbor, MI). Quercetin was obtained from Wako Pure Chemical Industries (Osaka, Japan). An enzyme-linked immunosorbent assay (ELISA) kit for mouse VEGF and an antibody against HSP70 (for immunoblotting analysis) were from R&D Systems (Minneapolis, MN). An antibody against HSP70 (for immunohistochemical analysis) was obtained from Stressgen (Ann Arbor, MI, USA). Antibodies against actin and BrdU were purchased from Santa Cruz Biotechnology (Santa Cruz, CA). An antibody against CD31, biotinylated anti-rat immunoglobulins and streptavidin-HRP were from BD Biosciences (San Jose, CA). Mayer's hematoxylin and malinol were from MUTO Pure Chemicals (Tokyo, Japan). The RNeasy kit was obtained from QIAGEN (Valencia, CA), the first-strand cDNA synthesis kit was from Takara (Kyoto, Japan), and iQ SYBR Green Supermix was from Bio-Rad (Hercules, CA). Transgenic mice expressing HSP70 and their wild-type counterparts (C57/BL6) were gifts from Drs. C.E. Angelidis and G.N. Pagoulatos (University of Ioannina, Ioannina, Greece) and were prepared (6–8 weeks of age and 20–25 g) as described previously [24]. Homozygotic male transgenic mice expressing HSP70 were used in these experiments. The experiments and procedures described here were performed in accordance with the Guide for the Care and Use of Laboratory Animals as adopted and promulgated by the National Institutes of Health, and were approved by the Animal Care Committee of Keio University.

2.2. Development of gastric ulcers

Gastric ulcers were produced by exposure of tissue to acetic acid according to a previously described method [25]. In brief, under ether anaesthesia, the abdomen was incised and the stomach exposed. A round plastic mold (4 mm in diameter) was placed on the serosal surface of the corpus and acetic acid (40%; 100 μl) was poured into the mold to treat the surface for 10 s. The treated surface was rinsed with saline, the abdomen was closed and the animals were routinely maintained. Control mice were operated in the same manner as the experimental group but not exposed to the acetic acid.

GGA (10 ml/kg as an emulsion with 5% gum arabic) was orally administered once only at day 0 (2 h before ulcer formation) once daily from day 3 to day 6 or day 8 (the ulcer was induced at day 0). We used 200 mg/kg doses of GGA, because this dose of GGA was shown to induce the expression of HSP70 clearly on our previous reports [5,6].

For measurement of gastric lesions, animals were sacrificed with an overdose of ether, after which their stomachs were removed and scored for hemorrhagic damage by an observer unaware of the treatment they had received. Calculation of the scores involved measuring the area of all lesions in millimetres squared and summing the values to give an overall gastric lesion index.

Gastric mucosal PGE_2 level was determined by EIA, as previously described [26]. The amount of VEGF in gastric tissue was measured by ELISA according to the manufacturer's protocol. For labeling with BrdU, BrdU (100 mg/kg) was injected intraperitoneally, 1 h before the mice were sacrificed, as described previously [27].

2.3. Real-time RT-PCR analysis

Total RNA was extracted from gastric tissue using an RNeasy kit according to the manufacturer's protocol. Samples (2.5 μg of RNA) were reverse-transcribed using a first-strand cDNA synthesis kit according to the manufacturer's instructions. Synthesized cDNA was used in real-time RT-PCR (Bio-Rad Chromo 4 system) experiments using iQ SYBR Green Supermix and analyzed with Opticon Monitor software according to the manufacturer's instructions. The real-time PCR cycle conditions were 95 °C for 3 min, followed by 44 cycles at 95 °C for 10 s and 60 °C for 60 s. Specificity was confirmed by electrophoretic analysis of the reaction products and by inclusion of template- or reverse transcriptase-free controls. To normalize the amount of total RNA present in each reaction, glyceraldehyde-3-phosphate dehydrogenase (GAPDH) cDNA was used as an internal standard.

Primers were designed using the Primer3 website. The primers used were (name, forward primer and reverse primer): bFGF: 5′-cccgacggccgcgtggat-3′, 5′-acttagaagccagcagccg-3′; IGF, 5′-gctggaccagagacccttttg-3′, 5′-gctccggaagcaacactca-3′; TGF-β1, 5′-tgacgtcactggagtacgg-3′, 5′-ggttcatgtcatggatggtgc-3′; GAPDH, 5′-aactttggcattgtggaagg-3′ and 5′-acacattggggtaggaaca-3′.

2.4. Immunohistochemical analysis

Gastric tissue samples were fixed in 10% buffered formalin and embedded in paraffin before being cut into 4 μm-thick sections.

For immunohistochemical analysis for HSP70 and BrdU, sections were incubated with 0.3% hydrogen peroxide in methanol for removal of endogenous peroxidase. For detection of BrdU, sections were treated in a microwave oven with 0.01 M citric acid buffer (pH 6.0) for antigen activation before the incubation with hydrogen peroxide. Sections were blocked with 3% BSA for 30 min,

incubated for 12 h with antibody against HSP70 (1:200 dilution) or BrdU (1:100 dilution) in the presence of 2.5% BSA, and then incubated for 1 h with peroxidase-labeled polymer conjugated to goat anti-mouse immunoglobulins. 3,3′-Diaminobenzidine was applied to the sections, which were incubated with Mayer's hematoxylin. Samples were mounted with malinol and inspected with the aid of a microscope (Olympus BX51).

For immunohistochemical analysis for CD31, sections were incubated with 0.3% hydrogen peroxide in methanol and then incubated with 20 μg/ml proteinase K for 20 min for antigen activation before blocking with 3% BSA for 30 min. Sections were incubated for 12 h with antibody against CD31 (1:50 dilution) in the presence of 2.5% BSA and then for 30 min with biotinylated anti-rat immunoglobulins. Sections were incubated for 30 min with streptavidin-HRP, following which 3,3′-diaminobenzidine was applied and the sections were finally incubated with Mayer's hematoxylin. Samples were mounted with malinol and inspected with the aid of a fluorescence microscope (Olympus BX51).

2.5. Immunoblotting analysis

Whole cell extracts were prepared as described previously [28]. The protein concentration of the sample was determined by the Bradford method [29]. Samples were applied to polyacrylamide SDS gels and subjected to electrophoresis, and the resultant proteins were immunoblotted with each antibody.

2.6. Purification of recombinant HSP70

The purification of His-tagged protein was performed as described previously [30]. The pET21 plasmid containing *hsp70* was introduced into *Escherichia coli* (BL21) cells and HSP70 was overproduced by incubation with 1 mM isopropyl-β-D-thiogalactopyranoside for 4 h at 30 °C. Cells were lysed by digestion with lysozyme in buffer A (50 mM NaH_2PO_4 (pH 8.0) and 0.5 M NaCl) containing 2 μg/ml pepstatin A, 1 mM benzamidine and 1 mM phenylmethylsulfonyl fluoride, and centrifuged. The supernatant was subjected to Ni-NTA agarose (Sigma) column chromatography, and HSP70 was eluted with buffer A containing 250 mM imidazole.

2.7. Statistical analysis

All values are expressed as the mean ± S.E.M. Two-way ANOVA followed by the Tukey test or a Student's *t* test for unpaired results was used to evaluate differences between more than three groups or between two groups, respectively. Differences were considered to be significant for values of $P < 0.05$.

3. Results

3.1. Alteration of gastric expression of HSP70 during ulcer healing

Changes in the gastric expression of HSP70 were examined for an acetic acid-induced ulcer during the healing process. The lesion

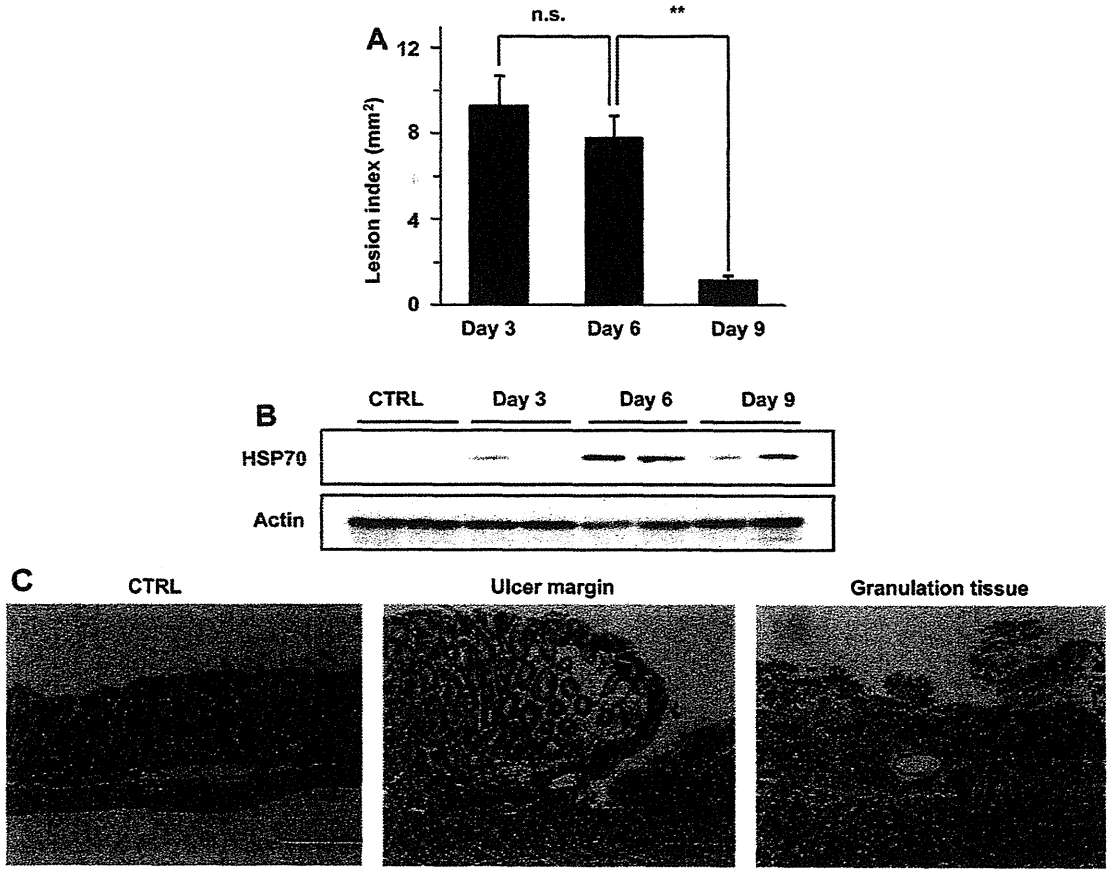

Fig. 1. Expression of HSP70 during gastric ulcer healing. Gastric ulcers were induced in wild-type mice by exposure of the luminal side of their stomachs to acetic acid at day 0, as described in Section 2, and the stomachs were removed at day 3, 6 or 9. Normal stomachs (without ulcer induction) (CTRL) were also prepared, as described in Section 2 (A–C). The stomachs were scored for hemorrhagic damage (A). Whole cell extracts were prepared from the stomachs and analyzed by immunoblotting with an antibody against HSP70 or actin (B). Sections of gastric tissues prepared at day 6 were subjected to immunohistochemical analysis with an antibody against HSP70 (C). Values are mean ± S.E.M. ($n = 3–5$) $^{**}P < 0.01$; n.s., not significant. Scale bar, 200 μm.

index decreased from day 3 to day 9 (Fig. 1A), showing that gastric ulcer healing progresses in this period. Immunoblotting analysis revealed that the expression of HSP70 was induced during this period of gastric ulcer healing (Fig. 1B). Immunohistochemical analysis with antibody against HSP70 revealed that induction of expression of HSP70 was observed both at the ulcer margin and in granulation tissue (Fig. 1C), suggesting that induced HSP70 plays an important role in gastric ulcer healing.

3.2. Effect of expression of HSP70 on gastric ulcer healing

In order to understand the role of HSP70 in gastric ulcer healing, we compared the progression of gastric ulcer healing in transgenic mice expressing HSP70 and in wild-type mice. As shown in Fig. 2A, the decrease in the lesion index after the development of a gastric ulcer was more rapid in the transgenic mice than in the wild-type mice. By immunoblotting analysis, we confirmed that HSP70 was expressed at high levels in the stomach in both control transgenic mice and in transgenic mice in which ulcers had been induced (Fig. 2B and C). These results suggest that expression of HSP70 accelerates gastric ulcer healing.

Cell proliferation at the gastric ulcer margin is important for gastric ulcer healing. To examine the effect of expression of HSP70 on cell proliferation at the gastric ulcer margin, we compared the number of BrdU-positive cells (proliferating cells) in transgenic mice expressing HSP70 and in wild-type mice by immunohistochemical analysis. The number of BrdU-positive cells at the gastric ulcer margin was higher in transgenic mice expressing HSP70 than in wild-type mice (Fig. 2D and E), suggesting that expression of HSP70 stimulates cell proliferation at the gastric ulcer margin. On the other hand, the background level of cell proliferation, that is in the absence of ulcer development, was indistinguishable between the wild-type and transgenic mice (Fig. 2D and E).

Angiogenesis in granulation tissue is also important for gastric ulcer healing. To examine the effect of expression of HSP70 on angiogenesis in granulation tissue, we compared the number of vessels by monitoring the expression of CD31, a marker for vascular endothelial cells between transgenic mice expressing HSP70 and in wild-type mice. In both types of mice, the number of vessels was higher in granulation tissue than in normal tissue (from mice without gastric ulcers), confirming that there was a higher level of angiogenesis in the granulation tissue (Fig. 2F and G). Furthermore, the number of vessels in the granulation tissue was higher in transgenic mice expressing HSP70 than in wild-type mice (Fig. 2F and G), suggesting that expression of HSP70 stimulates angiogenesis in granulation tissue. Again, the background number of vessels was similar for the different types of mouse (Fig. 2F and G).

The results in Fig. 2 suggest that expression of HSP70 accelerates gastric ulcer healing through stimulation of cell proliferation at the gastric ulcer margin and angiogenesis in granulation tissue. In order to understand the molecular mechanism, we examined the effect of the expression of HSP70 on the expression of growth factors, which stimulate cell proliferation at the gastric ulcer margin and angiogenesis in granulation tissue. As shown in Fig. 3A, the expression of bFGF, IGF and TGF-β1 mRNAs in the stomach was induced in ulcerated tissues, with the extent of induction being significantly greater in transgenic mice expressing HSP70 compared to wild-type mice. The gastric level of PGE_2 was also elevated in ulcerated tissues and the magnitude of this elevation was significantly greater in transgenic mice expressing HSP70 than in wild-type mice (Fig. 3B). We also found that the level of VEGF in ulcerated tissues was higher in transgenic mice than in wild-type mice (Fig. 3B). These results suggest that the high levels of these growth factors and PGE_2 are responsible for the observed HSP70-dependent acceleration of gastric ulcer healing.

3.3. Effect of GGA on gastric ulcer healing

As described in Section 1, GGA, a clinically used anti-ulcer drug, is an HSP-inducer. Thus, the results described above suggest that administration of GGA could stimulate gastric ulcer healing through the induction of HSP70 expression.

To test this idea, we first focused on HSP70 produced after the development of gastric ulcers, and therefore once daily administration of GGA was started at day 3. As shown in Fig. 4A, the legion index was lower for mice treated with GGA than for non-treated mice at both days 6 and 8, showing that administration of GGA accelerates gastric ulcer healing. Immunoblot analysis confirmed that the expression of HSP70 was induced by the GGA (Fig. 4B and C). Immunohistochemical analysis revealed that a GGA-induced expression of HSP70 took place both at the gastric ulcer margin and

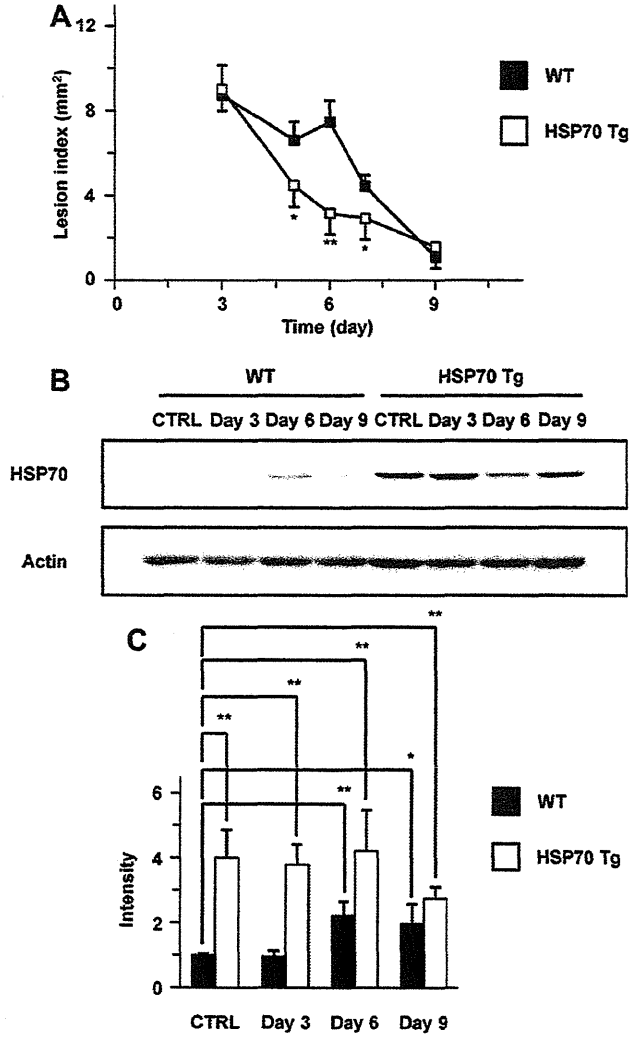

Fig. 2. Effect of expression of HSP70 on gastric ulcer healing. Gastric ulcers were induced in transgenic mice expressing HSP70 (HSP70 Tg) and wild-type mice (WT) as described in the legend of Fig. 1. (A–G). Hemorrhagic damage (A) and expression of HSP70 (B) were monitored as described in the legend of Fig. 1. The intensity of the HSP70 band was determined, normalized to that of actin and expressed relative to the control sample (C). Sections of gastric tissue were prepared at day 4 (D) or 6 (F) and subjected to immunohistochemical analysis with an antibody against BrdU (D) or CD31 (F). The lower panel in each group is a twice-magnified image of the boxed area in the higher panel (F). The ratio of BrdU-positive cells to total cells (200–400 cells) was determined (E). The number of vessels in a distinct area (0.09 mm^2) was counted (G). Values are mean ± S.E.M. ($n = 3–13$) $^{**}P < 0.01$; $^{*}P < 0.05$; n.s., not significant. Scale bar, 200 μm.

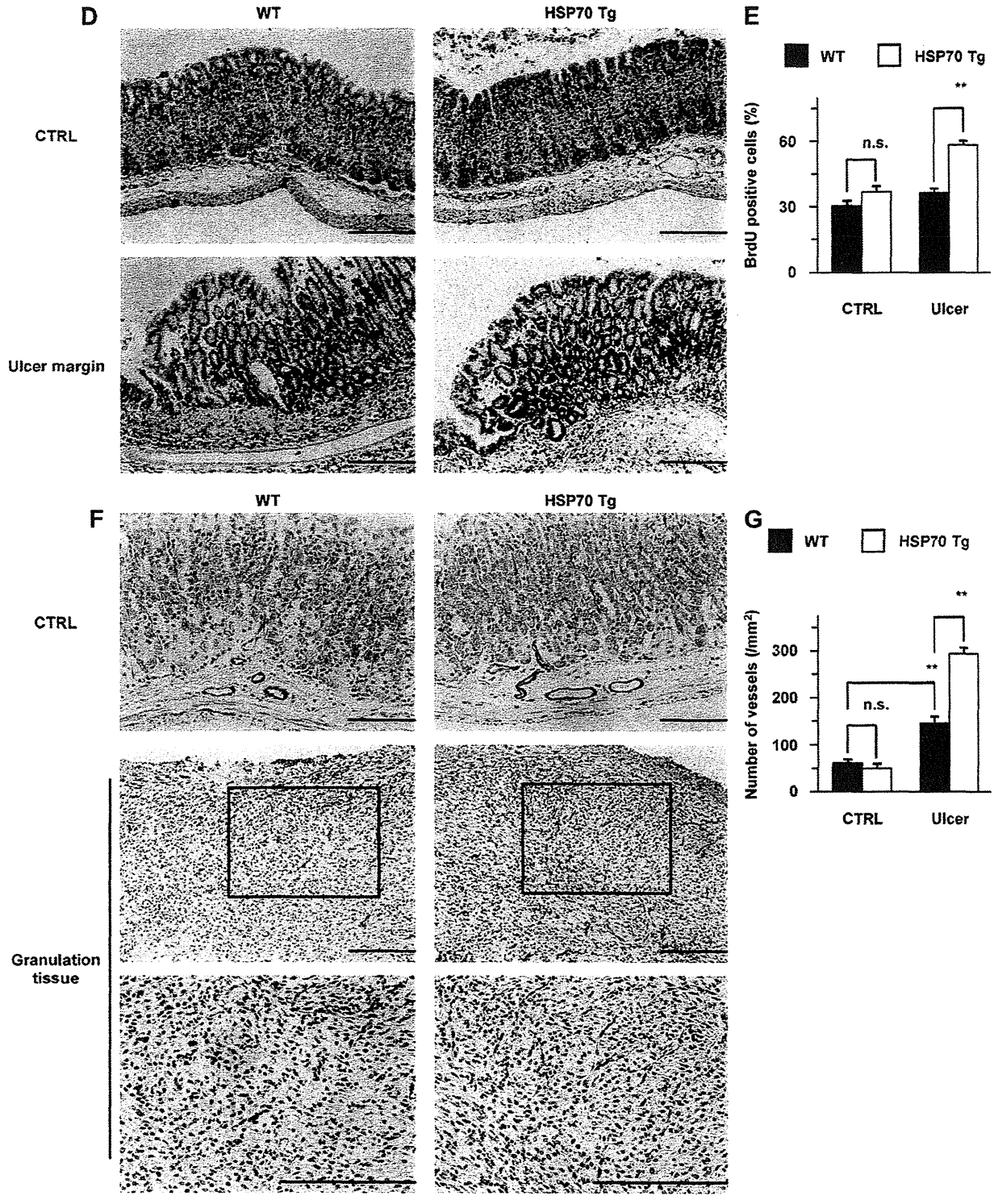

Fig. 2. (*Continued*).

in granulation tissue (Fig. 4D). To test the involvement of HSP70 in this stimulative effect of GGA on gastric ulcer healing, we examined the effect of pre-administration of quercetin (an inhibitor of expression of HSP70). As shown in Fig. 4E, pre-administration of quercetin diminished the stimulative effect of GGA on gastric ulcer healing, suggesting that GGA stimulates gastric ulcer healing through the induction of HSP70 expression. We also examined the effect of oral administration of purified recombinant HSP70 (from days 3 to 6) on gastric ulcer healing. This administration, however, did not affect the process (Fig. 4F).

We then focused our attention on HSP70 produced before the development of gastric ulcers since the background expression of

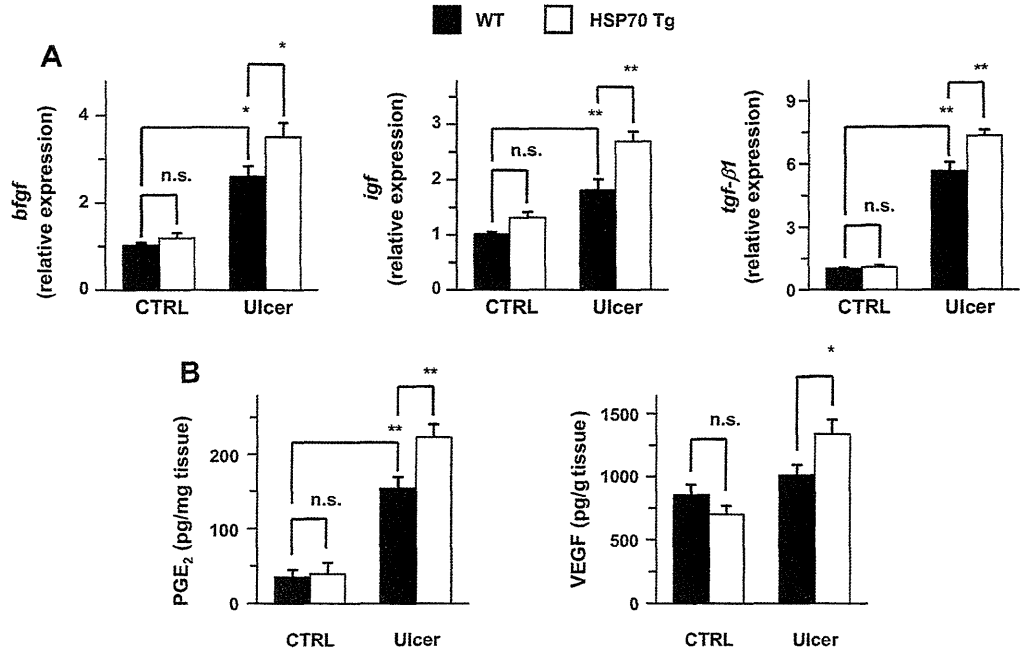

Fig. 3. Effect of expression of HSP70 on factors stimulating gastric ulcer healing. Gastric ulcers were induced in transgenic mice expressing HSP70 (HSP70 Tg) and wild-type mice (WT) as described in the legend of Fig. 1. (A and B) Total RNA was extracted at day 6 and subjected to real-time RT-PCR using a specific primer set for each gene. Values were normalized to the *gapdh* gene and expressed relative to the control sample (A). The gastric level of PGE_2 at day 3 or VEGF at day 6 was determined by EIA or ELISA, respectively (B). Values are mean ± S.E.M. ($n = 6–19$) $^{**}P < 0.01$; $^{*}P < 0.05$; n.s., not significant.

HSP70 in the absence of ulcers was also higher in the transgenic mice expressing HSP70 than in the wild-type mice. For this purpose, GGA was administered once only, 2 h before the induction of gastric ulcers. As shown in Fig. 5A, the legion index was lower for mice pre-treated with GGA than for un-treated mice at day 6 but not at day 3, showing that this administration of GGA also accelerated gastric ulcer healing but did not affect the development of gastric ulcers. Immunoblot and immunohistochemical analyses confirmed that GGA induced the expression of HSP70 at the gastric mucosa (Fig. 5B–D). Furthermore, in contrast to the results in Fig. 4F, oral administration of recombinant purified HSP70 (from day 0 to day 3) decreased the legion index at day 6 in a dose-dependent manner, showing that this administration stimulated gastric ulcer healing (Fig. 5E). To address the possibility that contaminated endotoxin but not HSP70 itself was responsible for this stimulation, the HSP70 fraction was denatured by boiling (100 °C for 1 h). It has previously been reported that this treatment diminishes the ability of HSP70, but not of endotoxin, to induce an innate immune response [15,16]. As shown in Fig. 5F, the boiled HSP70 fraction was inert for the stimulation of gastric ulcer healing. The results in Fig. 5 suggest that extracellular HSP70 is able to stimulate gastric ulcer healing.

4. Discussion

Identification of gastric mucosal defensive factors and understanding the molecular mechanisms underlying their actions are important in establishing clinical protocols for the treatment of gastric lesions. PGs, especially PGE_2, have been paid much attention as major defensive factors. HSP70 has also recently been identified as another major defensive factor. For the treatment of gastric ulcers it is important not only to prevent further ulcer formation, but also to enhance ulcer healing. It has been reported that PGE_2 not only prevents the formation of irritant-induced gastric ulcers but also enhances gastric ulcer healing [2,18,20]. As for HSP70, while it has become clear that expression of HSP70 prevents formation of irritant-induced gastric lesions, its role in gastric ulcer healing has been unclear. In this study, we have examined the role of HSP70 in gastric ulcer healing using transgenic mice expressing HSP70 and in response to treatment with GGA.

The expression of HSP70 was found to be induced during gastric ulcer healing. The induction was apparent at days 6 and 9, when ulcer healing progresses, and induction was observed both at the gastric ulcer margin and in granulation tissue, both of which are important regions for ulcer healing. These results suggest that this induction of expression of HSP70 plays an important role in gastric ulcer healing. Similar induction of expression of HSP70 during gastric ulcer healing has been reported elsewhere [31].

We found that gastric ulcer healing is accelerated in transgenic mice expressing HSP70, compared to wild-type mice. Furthermore, both cell proliferation at the gastric ulcer margin and angiogenesis in granulation tissue were accelerated in the transgenic mice. This is the first genetic evidence of a stimulative effect of HSP70 on gastric ulcer healing. Supporting this notion, we found that oral administration of GGA, an inducer of HSPs, stimulates gastric ulcer healing (see below). It was previously reported that pioglitazone, a specific ligand of peroxisome proliferator-activated receptor-gamma, accelerates gastric ulcer healing and induces expression of HSP70 in rats [32]. The results of this study could be extended to suggest that the HSP70 expression induced by pioglitazone is responsible for the acceleration of gastric ulcer healing induced by this drug.

As described in Section 1, increases in the gastric levels of PGE_2 and growth factors (such as bFGF, IGF, TGF-β1 and VEGF) accelerate gastric ulcer healing through enhancement of cell proliferation at the gastric ulcer margin and of angiogenesis in granulation tissue [17]. We have confirmed that expression of these growth factors (except VEGF), and the level of PGE_2, increase during gastric ulcer healing. We also found that these

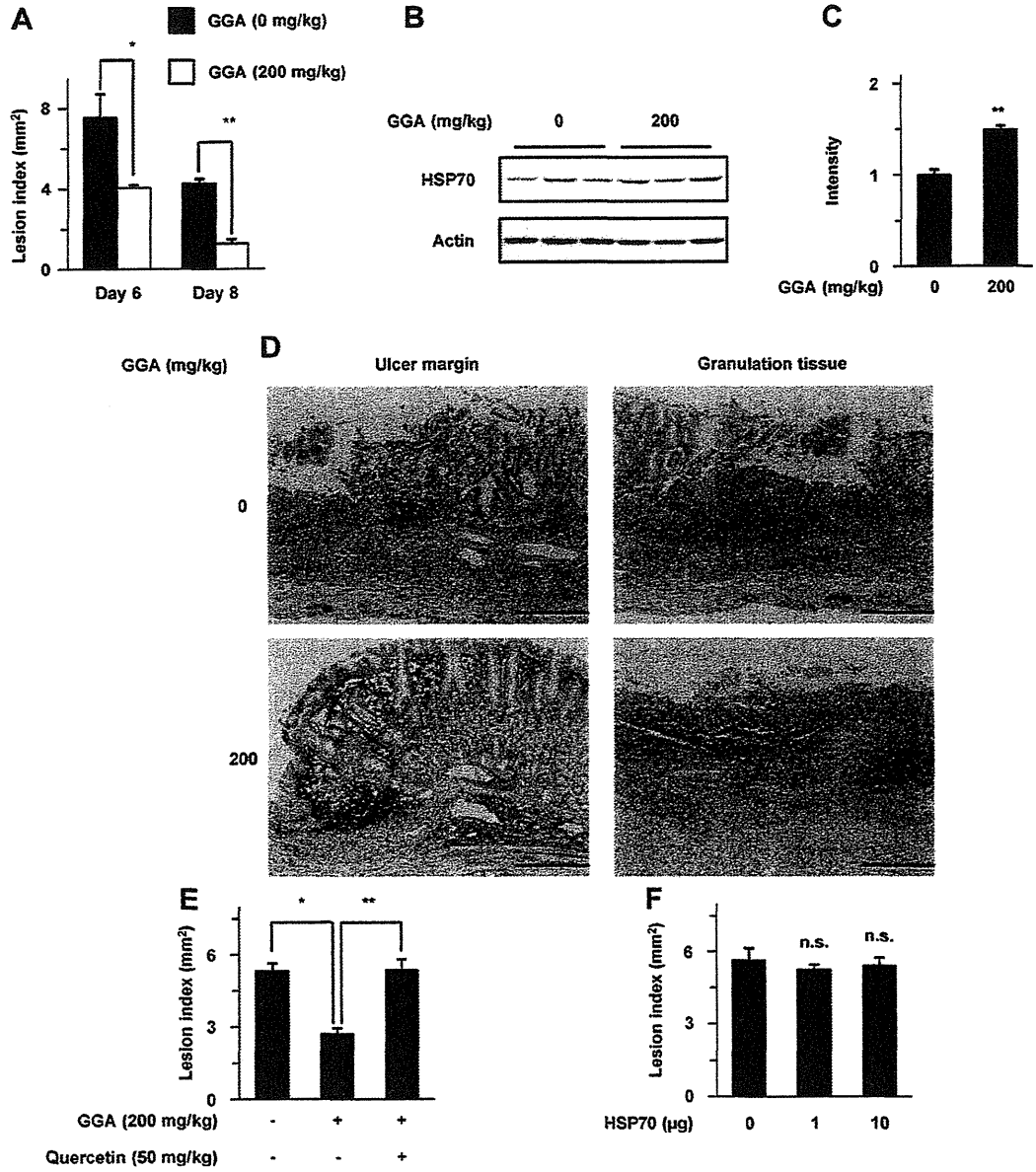

Fig. 4. Effect of GGA on expression of HSP70 and gastric ulcer healing. Gastric ulcers were induced in wild-type mice as described in the legend of Fig. 1. (A–F) Mice were orally administered 200 mg/kg of GGA (10 ml/kg as an emulsion with 5% gum arabic) once daily from day 3 to day 6 or day 8 (A). Mice were orally pre-administered 50 mg/kg of quercetin (10 ml/kg in water) 2 h before each GGA administration (E). Stomachs were removed 2 h after the final administration of GGA or purified HSP70, and hemorrhagic damage (A, E, F) and expression of HSP70 (B–D) monitored as described in the legend of Fig. 1. Values are mean ± S.E.M. (n = 3–7) $^{**}P < 0.01$; $^{*}P < 0.05$; n.s., not significant. Scale bar, 200 μm.

increases were further enhanced in transgenic mice expressing HSP70, suggesting that expression of HSP70 stimulates gastric ulcer healing by increasing the levels of these growth factors and PGE_2.

Both the background (without the development of gastric ulcers) and ulcer-induced expression of HSP70 were higher in transgenic mice expressing HSP70 than in wild-type mice. In order to evaluate the contribution of these HSP70 expression to the stimulation of gastric ulcer healing, we used the HSP70 inducer GGA, and found that its administration either prior to (at day 0) or after (from day 3) the development of gastric ulcers stimulated not only gastric expression of HSP70 but also gastric ulcer healing. These results suggest that both the background and ulcer-induced expression of HSP70 contributes to the stimulation of gastric ulcer healing in transgenic mice expressing HSP70. Furthermore, since HSP70 functions in both intracellular and extracellular compartments, we used the method of oral administration of purified HSP70 to examine the function of extracellular HSP70 in gastric ulcer healing. Administration of the protein from day 0 to day 3, but not from day 3 to day 6, stimulated gastric ulcer healing, suggesting that extracellular HSP70, that is HSP70 released from gastric cells, could enhance gastric ulcer healing at an early rather than a late stage. This idea is supported by the observation that administration of GGA but not purified HSP70 after the development of gastric ulcer stimulated the ulcer healing (Fig. 4A and F), because GGA may increase both intracellular and extracellular HSP70, however, administration of purified HSP may increase the only extracellular one.

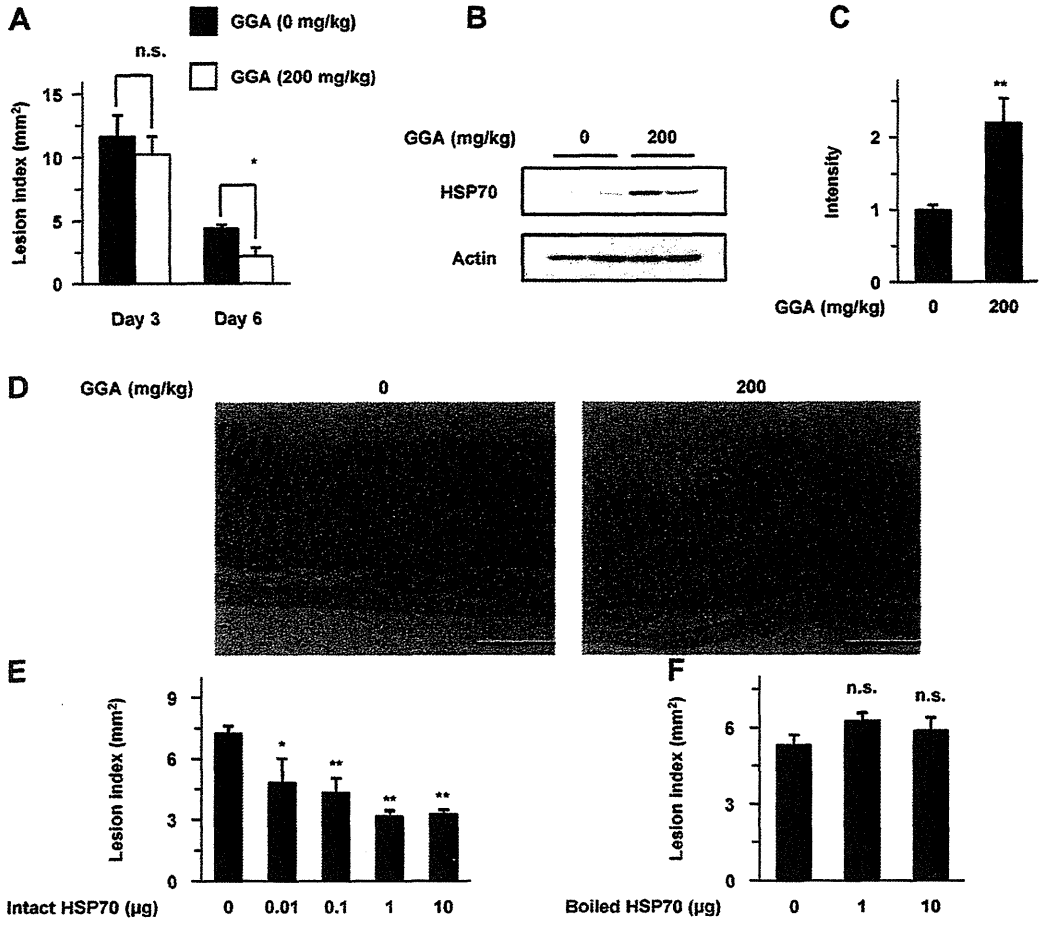

Fig. 5. Effect of GGA and HSP70 protein on gastric ulcer healing. Gastric ulcers were induced in wild-type mice as described in the legend of Fig. 1. (A–F) Mice were orally administered 200 mg/kg of GGA (10 ml/kg as an emulsion with 5% gum arabic) once only at day 0 (2 h before ulcer formation) (A–D). Mice were orally administered the indicated doses of intact purified recombinant HSP70 (E) or boiled HSP70 (F) (100 μl/mouse in PBS) once daily from day 0 to day 3. Stomachs were removed at day 0 (B–D, 2 h after the administration of GGA), day 3 (A) or day 6 (A, E, F), and hemorrhagic damage (A, E, F) and expression of HSP70 (B–D) were monitored as described in the legend of Fig. 1. Values are mean ± S.E.M. ($n = 3$–9) $^{**}P < 0.01$; $^{*}P < 0.05$; n.s., not significant. Scale bar, 200 μm.

In the early stages of gastric ulcer healing, the inflammatory response, which results in an increase in the level of PGE_2, induces expression of growth factors which stimulate cell proliferation at the gastric ulcer margin and angiogenesis in granulation tissue. Recent studies have revealed that extracellular HSP70 stimulates the innate immune response through its high-affinity receptors, including toll-like receptors, and activates nuclear factor kappa B [13–16]. It has also been reported that necrotic, but not apoptotic, cell death results in the release of intracellular HSPs [11,33]. Furthermore, although toll-like receptors play important roles in innate immunity, recent studies have revealed that their activation stimulates wound healing through various mechanisms including that via an increase in the levels of growth factors (such as VEGF) and the resulting activation of cell migration, proliferation and angiogenesis [34–38]. Thus we propose that HSP70 expressed at background levels (before the formation of a gastric ulcer) is released during the necrotic cell death associated with gastric ulcer formation to activate toll-like receptors, resulting in the stimulation of gastric ulcer healing. This notion is consistent with the idea that HSPs are major components of damage-associated molecular patterns (DAMPs), that are normally hidden in the interior of cells and are released from necrotic cells to stimulate the innate immune system [33].

In the late stages of ulcer healing, in addition to the stimulation of cell proliferation at the gastric ulcer margin and angiogenesis in granulation tissue, it is important to suppress the excessive inflammatory response and resulting cell death. Considering the cytoprotective and anti-inflammatory functions of intracellular HSP70, it is reasonable to speculate that HSP70 produced after the development of gastric ulcers does indeed stimulate gastric ulcer healing by suppressing these processes. The result also suggests that the induction of expression of HSP70 during gastric ulcer healing in wild-type mice contributes to gastric ulcer healing.

GGA was developed in 1984 as an anti-ulcer drug and a number of previous studies have revealed that GGA not only protects the gastric mucosa against irritant-induced lesions but also stimulates the ulcer healing process [39,40]. In addition to various gastroprotective actions, such as increasing gastric mucosal blood flow, stimulation of surface mucus production and direct protection of gastric mucosal cell membranes [41–43], we recently revealed that the HSP-inducing ability of GGA also contributes to the protective effect of GGA against irritant-induced gastric lesions [5,6]. In this study, we have shown that GGA enhances the expression of HSP70 in ulcerated tissues and improves gastric ulcer healing. Taken together with our results obtained with transgenic mice expressing HSP70, we propose that the HSP70-inducing ability of GGA contributes to its stimulative effect on gastric ulcer healing.

Acknowledgements

We thank Dr. H. Kido (University of Tokushima, Japan) for generously providing the pET21 plasmid containing *hsp70*. We also thank Drs. C.E. Angelidis and G.N. Pagoulatos (University of Ioannina, Greece) for generously providing the transgenic mice expressing HSP70.

This work was supported by Grants-in-Aid for Scientific Research from the Ministry of Health, Labour, and Welfare of Japan, as well as the Japan Science and Technology Agency and Grants-in-Aid for Scientific Research from the Ministry of Education, Culture, Sports, Science and Technology, Japan.

References

[1] Holzer P. Neural emergency system in the stomach. Gastroenterology 1998;114:823–39.
[2] Miller TA. Protective effects of prostaglandins against gastric mucosal damage: current knowledge and proposed mechanisms. Am J Physiol 1983;245: G601–23.
[3] Mathew A, Morimoto RI. Role of the heat-shock response in the life and death of proteins. Ann N Y Acad Sci 1998;851:99–111.
[4] Morimoto RI, Santoro MG. Stress-inducible responses and heat shock proteins: new pharmacologic targets for cytoprotection. Nat Biotechnol 1998;16:833–8.
[5] Tanaka K, Tsutsumi S, Arai Y, Hoshino T, Suzuki K, Takaki E, et al. Genetic evidence for a protective role of heat shock factor 1 against irritant-induced gastric lesions. Mol Pharmacol 2007;71:985–93.
[6] Suemasu S, Tanaka K, Namba T, Ishihara T, Katsu T, Fujimoto M, et al. A role for HSP70 in protecting against indomethacin-induced gastric lesions. J Biol Chem 2009;284:19705–1.
[7] Hirakawa T, Rokutan K, Nikawa T, Kishi K. Geranylgeranylacetone induces heat shock proteins in cultured guinea pig gastric mucosal cells and rat gastric mucosa. Gastroenterology 1996;111:345–57.
[8] Mizushima T, Tsutsumi S, Rokutan K, Tsuchiya T. Suppression of ethanol-induced apoptotic DNA fragmentation by geranylgeranylacetone in cultured guinea pig gastric mucosal cells. Dig Dis Sci 1999;44:510–4.
[9] Tomisato W, Takahashi N, Komoto C, Rokutan K, Tsuchiya T, Mizushima T. Geranylgeranylacetone protects cultured guinea pig gastric mucosal cells from indomethacin. Dig Dis Sci 2000;45:1674–9.
[10] Tomisato W, Tsutsumi S, Tsuchiya T, Mizushima T. Geranylgeranylacetone protects guinea pig gastric mucosal cells from gastric stressor-induced necrosis by induction of heat-shock proteins. Biol Pharm Bull 2001;24:887–91.
[11] Basu S, Binder RJ, Suto R, Anderson KM, Srivastava PK. Necrotic but not apoptotic cell death releases heat shock proteins, which deliver a partial maturation signal to dendritic cells and activate the NF-kappa B pathway. Int Immunol 2000;12:1539–46.
[12] Bausero MA, Gastpar R, Multhoff G, Asea A. Alternative mechanism by which IFN-gamma enhances tumor recognition: active release of heat shock protein 72. J Immunol 2005;175:2900–12.
[13] Asea A, Kraeft SK, Kurt-Jones EA, Stevenson MA, Chen LB, Finberg RW, et al. HSP70 stimulates cytokine production through a CD14-dependant pathway, demonstrating its dual role as a chaperone and cytokine. Nat Med 2000;6:435–42.
[14] Calderwood SK, Mambula SS, Gray Jr PJ, Theriault JR. Extracellular heat shock proteins in cell signaling. FEBS Lett 2007;581:3689–94.
[15] Asea A, Rehli M, Kabingu E, Boch JA, Bare O, Auron PE, et al. Novel signal transduction pathway utilized by extracellular HSP70: role of toll-like receptor (TLR) 2 and TLR4. J Biol Chem 2002;277:15028–34.
[16] Chase MA, Wheeler DS, Lierl KM, Hughes VS, Wong HR, Page K. Hsp72 induces inflammation and regulates cytokine production in airway epithelium through a TLR4- and NF-kappaB-dependent mechanism. J Immunol 2007;179:6318–24.
[17] Tarnawski AS. Cellular and molecular mechanisms of gastrointestinal ulcer healing. Dig Dis Sci 2005;50(Suppl. 1):S24–33.
[18] Hatazawa R, Tanaka A, Tanigami M, Amagase K, Kato S, Ashida Y, et al. Cyclooxygenase-2/prostaglandin E2 accelerates the healing of gastric ulcers via EP4 receptors. Am J Physiol Gastrointest Liver Physiol 2007;293:G788–97.
[19] Takahashi S, Shigeta J, Inoue H, Tanabe T, Okabe S. Localization of cyclooxygenase-2 and regulation of its mRNA expression in gastric ulcers in rats. Am J Physiol 1998;275:G1137–45.
[20] Konturek SJ, Konturek PC, Brzozowski T. Prostaglandins and ulcer healing. J Physiol Pharmacol 2005;56(Suppl. 5):5–31.
[21] Wong WM, Playford RJ, Wright NA. Peptide gene expression in gastrointestinal mucosal ulceration: ordered sequence or redundancy? Gut 2000;46:286–92.
[22] Milani S, Calabro A. Role of growth factors and their receptors in gastric ulcer healing. Microsc Res Tech 2001;53:360–71.
[23] Szabo S, Folkman J, Vattay P, Morales RE, Pinkus GS, Kato K. Accelerated healing of duodenal ulcers by oral administration of a mutein of basic fibroblast growth factor in rats. Gastroenterology 1994;106:1106–11.
[24] Tanaka K, Namba T, Arai Y, Fujimoto M, Adachi H, Sobue G, et al. Genetic evidence for a protective role for heat shock factor 1 and heat shock protein 70 against colitis. J Biol Chem 2007;282:23240–52.
[25] Okabe S, Amagase K. An overview of acetic acid ulcer models – the history and state of the art of peptic ulcer research. Biol Pharm Bull 2005;28:1321–41.
[26] Futaki N, Arai I, Hamasaka Y, Takahashi S, Higuchi S, Otomo S. Selective inhibition of NS-398 on prostanoid production in inflamed tissue in rat carrageenan-air-pouch inflammation. J Pharm Pharmacol 1993;45:753–5.
[27] Kabashima K, Saji T, Murata T, Nagamachi M, Matsuoka T, Segi E, et al. The prostaglandin receptor EP4 suppresses colitis, mucosal damage and CD4 cell activation in the gut. J Clin Invest 2002;109:883–93.
[28] Hoshino T, Tsutsumi S, Tomisato W, Hwang HJ, Tsuchiya T, Mizushima T. Prostaglandin E2 protects gastric mucosal cells from apoptosis via EP2 and EP4 receptor activation. J Biol Chem 2003;278:12752–8.
[29] Bradford MM. A rapid and sensitive method for the quantitation of microgram quantities of protein utilizing the principle of protein–dye binding. Anal Biochem 1976;72:248–54.
[30] Asano T, Makise M, Takehara M, Mizushima T. Interaction between ORC and Cdt1p of *Saccharomyces cerevisiae*. FEMS Yeast Res 2007;7:1256–62.
[31] Tsukimi Y, Nakai H, Itoh S, Amagase K, Okabe S. Involvement of heat shock proteins in the healing of acetic acid-induced gastric ulcers in rats. J Physiol Pharmacol 2001;52:391–406.
[32] Konturek PC, Brzozowski T, Kania J, Konturek SJ, Kwiecien S, Pajdo R, et al. Pioglitazone, a specific ligand of peroxisome proliferator-activated receptor-gamma, accelerates gastric ulcer healing in rat. Eur J Pharmacol 2003;472:213–20.
[33] Kono H, Rock KL. How dying cells alert the immune system to danger. Nat Rev Immunol 2008;8:279–89.
[34] West XZ, Malinin NL, Merkulova AA, Tischenko M, Kerr BA, Borden EC, et al. Oxidative stress induces angiogenesis by activating TLR2 with novel endogenous ligands. Nature 2010;467:972–6.
[35] Macedo L, Pinhal-Enfield G, Alshits V, Elson G, Cronstein BN, Leibovich SJ. Wound healing is impaired in MyD88-deficient mice: a role for MyD88 in the regulation of wound healing by adenosine A2A receptors. Am J Pathol 2007;171:1774–88.
[36] Sato T, Yamamoto M, Shimosato T, Klinman DM. Accelerated wound healing mediated by activation of Toll-like receptor 9. Wound Repair Regen 2010;18:586–93.
[37] Pollet I, Opina CJ, Zimmerman C, Leong KG, Wong F, Karsan A. Bacterial lipopolysaccharide directly induces angiogenesis through TRAF6-mediated activation of NF-kappaB and c-Jun N-terminal kinase. Blood 2003;102:1740–2.
[38] Grote K, Schuett H, Salguero G, Grothusen C, Jagielska J, Drexler H, et al. Toll-like receptor 2/6 stimulation promotes angiogenesis via GM-CSF as a potential strategy for immune defense and tissue regeneration. Blood 2010;115: 2543–52.
[39] Kobayashi T, Ohta Y, Yoshino J, Nakazawa S. Teprenone promotes the healing of acetic acid-induced chronic gastric ulcers in rats by inhibiting neutrophil infiltration and lipid peroxidation in ulcerated gastric tissues. Pharmacol Res 2001;43:23–30.
[40] Ito M, Tanaka T, Suzuki Y. Increasing action of teprenone, a new antiulcer agent, on high-molecular-weight glycoprotein in gastric mucus during the healing process of acetic acid-induced ulcer in rats. Jpn J Pharmacol 1986;41:117–25.
[41] Terano A, Hiraishi H, Ota S, Sugimoto T. Geranylgeranylacetone, a novel anti-ulcer drug, stimulates mucus synthesis and secretion in rat gastric cultured cells. Digestion 1986;33:206–10.
[42] Kunisaki C, Sugiyama M. Effect of teprenone on acute gastric mucosal lesions induced by cold-restraint stress. Digestion 1992;53:45–53.
[43] Ushijima H, Tanaka K, Takeda M, Katsu T, Mima S, Mizushima T. Geranylgeranylacetone protects membranes against nonsteroidal anti-inflammatory drugs. Mol Pharmacol 2005;68:1156–61.

Suppression of Expression of Heat Shock Protein 70 by Gefitinib and Its Contribution to Pulmonary Fibrosis

Takushi Namba[1], Ken-Ichiro Tanaka[1], Tatsuya Hoshino[1], Arata Azuma[2], Tohru Mizushima[1,3]*

1 Graduate School of Medical and Pharmaceutical Sciences, Kumamoto University, Kumamoto, Japan, **2** Division of Respiratory, Infection and Oncology, Department of Internal Medicine, Nippon Medical School, Tokyo, Japan, **3** Department of Analytical Chemistry, Faculty of Pharmacy, Keio University, Tokyo, Japan

Abstract

Drug-induced interstitial lung disease (ILD), particularly pulmonary fibrosis, is of serious clinical concern. Gefitinib, a tyrosine kinase inhibitor of the epidermal growth factor receptor (EGFR), is beneficial as a drug for treating non-small cell lung cancer; however, this drug induces ILD and the molecular mechanisms underpinning this condition remain unclear. We recently reported that expression of heat shock protein 70 (HSP70) protects against bleomycin-induced pulmonary fibrosis, an animal model of pulmonary fibrosis. In this study, we have examined the effects of drugs known to induce ILD clinically on the expression of HSP70 in cultured lung epithelial cells and have found that gefitinib has a suppressive effect. Results of a luciferase reporter assay, pulse-labelling analysis of protein and experiments using an inhibitor of translation or transcription suggest that gefitinib suppresses the expression of HSP70 at the level of translation. Furthermore, the results of experiments with siRNA for Dicer1, an enzyme responsible for synthesis of microRNA, and real-time RT-PCR analysis suggest that some microRNAs are involved in the gefitinib-induced translational inhibition of HSP70. Mutations in the EGFR affect the concentration of gefitinib required for suppressing the expression of HSP70. These results suggest that gefitinib suppresses the translation of HSP70 through an EGFR- and microRNA-mediated mechanism. *In vivo*, while oral administration of gefitinib suppressed the pulmonary expression of HSP70 and exacerbated bleomycin-induced pulmonary fibrosis in wild-type mice, these effects were not as distinct in transgenic mice expressing HSP70. Furthermore, oral co-administration of geranylgeranylacetone (GGA), an inducer of HSP70, suppressed gefitinib-induced exacerbation of bleomycin-induced pulmonary fibrosis. Taken together, these findings suggest that gefitinib-induced exacerbation of bleomycin-induced pulmonary fibrosis is mediated by suppression of pulmonary expression of HSP70 and that an inducer of HSP70 expression, such as GGA, may be therapeutically beneficial for the treatment of gefitinib-induced pulmonary fibrosis.

Citation: Namba T, Tanaka K-I, Hoshino T, Azuma A, Mizushima T (2011) Suppression of Expression of Heat Shock Protein 70 by Gefitinib and Its Contribution to Pulmonary Fibrosis. PLoS ONE 6(11): e27296. doi:10.1371/journal.pone.0027296

Editor: Kaustubh Datta, University of Nebraska Medical Center, United States of America

Received August 10, 2011; **Accepted** October 13, 2011; **Published** November 9, 2011

Funding: This work was supported by Grants-in-Aid of Scientific Research from the Ministry of Health, Labour, and Welfare of Japan (http://www.mhlw.go.jp/english/index.html), Grants-in-Aid for Scientific Research from the Ministry of Education, Culture, Sports, Science and Technology of Japan (http://www.mext.go.jp/), and Grants-in-Aid of the Japan Science and Technology Agency (http://www.jst.go.jp/). The funders had no role in study design, data collection and analysis, decision to publish, or preparation of the manuscript.

Competing Interests: The authors have declared that no competing interests exist.

* E-mail: mizu@gpo.kumamoto-u.ac.jp

Introduction

Interstitial lung disease (ILD), in particular interstitial pneumonia associated with pulmonary fibrosis, is a devastating chronic lung condition with poor prognosis. Pulmonary fibrosis progresses insidiously, with acute exacerbation of interstitial pneumonia being a highly lethal clinical event [1], [2]. Although most cases of pulmonary fibrosis are idiopathic, some are due to drug side effects (drug-induced pulmonary fibrosis). For example, the anti-tumour drugs gefitinib and imatinib, as well as anti-rheumatoid arthritis drugs such as leflunomide, are known to induce ILD (pulmonary fibrosis). This is cause for serious clinical concern, as it restricts the therapeutic use of these drugs [3], [4], [5]. Unfortunately, the etiology of drug-induced ILD (pulmonary fibrosis) is not yet understood and, as a result, an appropriate animal model has not yet been established. Understanding the mechanism governing drug-induced ILD (pulmonary fibrosis) and developing a viable animal model are therefore important to establish not only a clinical protocol for its treatment but also an assay system that will facilitate screening in order to eliminate candidate drugs with the potential to produce this type of side effect. Bleomycin-induced pulmonary fibrosis in animals mimics some characteristics of human pulmonary fibrosis [6]. We recently reported that leflunomide exacerbates bleomycin-induced pulmonary fibrosis, proposed that this model is a suitable animal model for drug-induced ILD, and suggested that this exacerbation is mediated by epithelial-mesenchymal transition (EMT) of lung epithelial cells [7]. However, the molecular mechanisms underpinning ILD (pulmonary fibrosis) induced by drugs other than leflunomide remain unclear.

Pulmonary fibrosis is induced by repeated epithelial cell damage by reactive oxygen species (ROS) and other stressors and abnormal wound repair and remodelling, resulting in abnormal deposition of extracellular matrix (ECM) proteins, such as collagen. In addition to the increase in transforming growth factor (TGF)-β1 [8], an increase in the level of lung myofibroblasts has been suggested to play an important role in pulmonary fibrosis [9]. It was previously believed that the sole origin of myofibroblasts is

peribronchiolar and perivascular fibroblasts that transdifferentiate into myofibroblasts [10]. However, recently, it was revealed that some of the lung myofibroblasts in pulmonary fibrosis patients originate from lung epithelial cells via EMT [11], [12], [13], [14].

Gefitinib, a tyrosine kinase inhibitor of the epidermal growth factor receptor (EGFR), is a new molecular target agent for the treatment of patients with advanced non-small cell lung cancer who fail to respond to chemotherapy [15]. Furthermore, recent clinical studies have shown that this drug is particularly effective for patients with EGFR mutations, which causes constitutive activation of EGFR-dependent intracellular signal transduction [16], [17]. Although gefitinib has been recognised as relatively safe based on data from clinical trials, post-marketing surveillance of patients prescribed with gefitinib in Japan has revealed that 6.8% of patients developed interstitial pneumonia and that, of these, 40% of the patients died [4], [18], [19]. The incidence of gefitinib-induced ILD and its mortality rate are higher in Japan than in Western countries [20], [21]. However, the mechanism governing gefitinib-induced ILD (pulmonary fibrosis) and the reason for this ethnic difference is unknown. Furthermore, contradictory results have been reported regarding the effect of gefitinib on bleomycin-induced pulmonary fibrosis in animals (prevention and exacerbation) [22], [23] and the mechanisms governing these phenomena are unknown.

Different stressors induce cells to express heat shock proteins (HSPs) through transcriptional regulation mediated by a transcription factor, heat shock factor 1 (HSF1), and a *cis*-element located in the *hsp* gene promoter, heat shock element (HSE) [24]. HSPs, especially HSP70, expressed in cultured cells protect these cells against a range of stressors, including ROS, by refolding or degrading denatured proteins produced by the stressors (HSPs function as molecular chaperones) [24], [25]. Interestingly, geranylgeranylacetone (GGA), a leading anti-ulcer drug on the Japanese market, has been reported to be a non-toxic HSP-inducer [26], [27]. In addition to the cytoprotective effects of HSP70, its anti-inflammatory effects have been identified recently [28]. We have shown that through the cytoprotective, anti-inflammatory and molecular chaperone activities, both genetic and pharmacologic (by GGA) induction of expression of HSP70 is protective in animal models of various diseases, such as gastric and small intestinal lesions, inflammatory bowel diseases, ultraviolet light-induced skin damage and Alzheimer's disease [29], [30], [31], [32], [33], [34]. Furthermore, we recently reported that bleomycin-induced lung injury, inflammation, fibrosis and dysfunction are suppressed in transgenic mice expressing HSP70 or in GGA-administered wild-type mice. We also suggested that HSP70 plays this protective role through cytoprotective and inflammatory effects and by inhibiting the production of TGF-β1 and TGF-β1-dependent EMT of lung epithelial cells [35].

As a mechanism for the regulation of gene expression, microRNAs (miRNAs) have been paid much attention recently. miRNAs are short non-coding single-stranded RNA species which bind to complementary regions of the 3' untranslated regions (UTRs) of mRNA resulting in repression of translation and/or stimulation of degradation of mRNA. Primary miRNA transcripts are first processed in the nucleus to produce hairpin RNAs (pre-miRNAs), which are then exported into the cytoplasm, where Dicer1 cuts the hairpin to produce miRNAs [36]. Aberrant expression of miRNAs is associated with pathologic conditions, such as cancer, diabetes and fibrosis [36,37].

In this study, we examined the effect on the expression of HSP70 of drugs known to induce ILD clinically in cultured lung epithelial cells, and found that gefitinib suppresses the expression of HSP70. The results suggest that gefitinib regulates expression of HSP70 at the level of translation through an EGFR- and miRNA-mediated mechanism. We also found that oral administration of gefitinib suppresses pulmonary expression of HSP70 and suggested that this suppression is involved in gefitinib-induced exacerbation of bleomycin-induced pulmonary fibrosis. These results suggest that HSP70 plays an important role in gefitinib-induced ILD (pulmonary fibrosis) and that examination of the effect of drugs on HSP70-expression *in vitro* is useful as a screening system in order to eliminate candidate drugs with the potential to induce ILD.

Materials and Methods

Ethics Statement

The experiments and procedures described here were carried out in accordance with the Guide for the Care and Use of Laboratory Animals as adopted and promulgated by the National Institutes of Health, and were approved by the Animal Care Committee of Kumamoto University. Permit numbers or approval ID for this study is C-20–166-R1.

Chemicals and animals

Paraformaldehyde, fetal bovine serum (FBS), 4-(dimethylamino)-benzaldehyde (DMBA), chloramine T, cycloheximide, SP600125, Orange G, RPMI1640 and DMEM were obtained from Sigma (St. Louis, MO). Bleomycin was purchased from Nippon Kayaku (Tokyo, Japan). An RNeasy kit, miScript miRNA Mimic and HiPerFect were obtained from Qiagen (Valencia, CA), the PrimeScript® 1st strand cDNA synthesis kit was from TAKARA Bio (Ohtsu, Japan), and the iQ SYBR Green Supermix was from Bio-Rad (Hercules, CA). The mirVana miRNA isolation kit and pMIR-REPORT System were purchased from Applied Biosystems (Carlsbad, CA). Antibodies against actin and HSP70 were purchased from Santa Cruz Biotechnology, Inc. (Santa Cruz, CA) and BD Bioscience (San Francisco, CA), respectively. Antibodies against HSP27, HSP47, HSP60 and HSP90 were from Stressgene (San Francisco, CA). The NCode VILO miRNA cDNA synthesis kit and Lipofectamine (TM2000) were obtained from Invitrogen (Carlsbad, CA). A771726, gefitinib, imatinib, amiodarone, L-hydroxyproline, azophloxin and aniline blue were from WAKO Pure Chemicals (Tokyo, Japan). Xylidine ponceau was from WALDECK GmbH & Co. (Muenster, Germany), and Mayer's hematoxylin, 1% eosin alcohol solution, mounting medium for histological examination (malinol) and Weigert's iron hematoxylin were from MUTO Pure Chemicals (Tokyo, Japan). Transgenic mice expressing HSP70 were gifts from Drs. CE Angelidis and GN Pagoulatos (University of Ioannina, Ioannina, Greece) and were crossed with C57BL/6J wild-type mice 10 times to generate the mice used in this study [32].

Cell culture

A549 and H1975 cells, and PC9 cells were cultured in DMEM and RPMI1640 medium, respectively, supplemented with 10% FBS, 100 U/ml penicillin and 100 μg/ml streptomycin in a humidified atmosphere of 95% air with 5% CO_2 at 37°C.

Real-time RT-PCR analysis

Real-time RT-PCR was performed as previously described [38] with some modifications. Total RNA was extracted from cells using an RNeasy kit or mirVana miRNA isolation kit according to the manufacturer's protocol. Samples were reverse-transcribed using a first-strand cDNA synthesis kit or NCode VILO miRNA cDNA synthesis kit. Synthesized cDNA was used in real-time RT-PCR experiments (Chromo 4 instrument; Bio-Rad Laboratories) using iQ SYBR GREEN Supermix, and analyzed with Opticon

Monitor Software. Specificity was confirmed by electrophoretic analysis of the reaction products and by the inclusion of template- or reverse transcriptase-free controls. To normalize the amount of total RNA present in each reaction, *actin* or RUN44 cDNA was used as an internal standard. Primers were designed using the Primer3 website or NCode™ miRNA database website.

The primers used were (name: forward primer, reverse primer): *hsp27*: 5'-ccacccaagtttcctcctc-3', 5'-gactgggatggtgatctcgt-3'; *hsp47*: 5'-ccatgttcttcaagccacact-3', 5'-cgtagtagttgtagaggcctgt-3'; *hsp60*: 5'-tttcagatggagtggctgtg-3', 5'-caatgccttcttcaacagca-3'; *hsp70*: 5'-aggccaacaagatcaccatc-3', 5'-tcgtcctccgctttgtactt-3'; *hsp90*: 5'-ggcagaggctgataagaacg-3', 5'-ctggggatcttccagactga-3'; *actin*: 5'-ggacttcgagcaagagatgg-3', 5'- agcactgtgttggcgtacag-3'; miR-146a: 5'-tgagaactgaattccatgggtt-3'; miR-146b-5p: 5'-gtgagaactgaattccataggct-3'; miR-223*: 5'-gcgtgtatttgacaagctgagtt-3'; miR-561: 5'-cgcaaagtttaagatccttgaagt-3'; miR-449a: 5'-tggcagtgtattgttagctggt-3'; miR-449b: 5'-aggcagtgtattgttagctggc-3'; RUN44: 5'-gagctaattaagaccttcatgttca-3', 5'-cctggatgatgataagcaaatg-3'. For miRNAs, the universal primer in the NCode VILO miRNA cDNA synthesis kit was used as the reverse primer.

We searched for miRNAs that potentially bind to the 3' UTR of *hsp70*, using the TargetScan and Segal Lab websites.

Luciferase assay

DNA fragments of the *hsp70* 3' UTR (from 2169 to 2427) were amplified by PCR and ligated into the Spe*I*-Hin*dIII* site of the *Photinus pyralis* luciferase reporter plasmid (pMIR-REPORT) to generate pMIR/luc/*hsp70* 3' UTR. The pGL-3/HSE plasmid was constructed by inserting HSE just upstream of the *luciferase* gene. The pGL-3/*hsp70*pro plasmid, which was constructed by inserting the *hsp70* promoter into the same region, was generously provided by Dr. Chang EB (University of Chicago). The luciferase assay was performed as described previously [38]. Transfections were carried out using Lipofectamine (TM2000) according to the manufacturer's instructions. Cells were used for experiments after a 24 h recovery period. Transfection efficiency was determined in parallel plates by transfection of cells with a pEGFP-N1 control vector. Cells were transfected with 0.5 μg of one of the *Photinus pyralis* luciferase reporter plasmids (pMIR/luc/*hsp70* 3' UTR, pGL-3/*hsp70*pro or pGL-3/HSE) and 0.125 μg of the internal standard plasmid bearing the *Renilla reniformis* luciferase reporter (pRL-SV40). *Photinus pyralis* luciferase activity in the cell extracts was measured using the Dual Luciferase Assay System and then normalized for *Renilla reniformis* luciferase activity.

Immunoblotting analysis

Whole cell extracts were prepared as described previously [38]. The protein concentration of the samples was determined by the Bradford method [39]. Samples were applied to polyacrylamide SDS gels, subjected to electrophoresis, and the resultant proteins immunoblotted with their respective antibodies.

Pulse-chase and pulse-labelling analyses

Pulse-chase and pulse-labelling analyses were carried out as described previously [40], with some modifications. Cells were labelled with [^{35}S]methionine and [^{35}S]cysteine in methionine- and cysteine-free RPMI1640 medium for 15 min. To chase labelled proteins, cells were washed with fresh complete (with methionine and cysteine) medium three times and incubated in complete medium for 4 or 8 h. HSP70 was immunoprecipitated with its antibody and separated by SDS-polyacrylamide gel electrophoresis, and visualised by autoradiography (Fuji BAS 2500 imaging analyzer).

Transfection of cells with siRNA or miRNA mimic RNA fragments

The siRNA for Dicer1 and the miRNA mimic RNA fragments for miR-146a and miR-146b-5p were purchased from Qiagen. A549 cells were transfected with these RNAs using HiPerFect transfection reagents according to the manufacturer's instructions. The siRNA (5'-uucuccgaacgugucacgudTdT-3' and 5'-acgugacacguucggagaadTdT-3') was used as a non-specific siRNA.

Administration of bleomycin, gefitinib and GGA

C57BL/6 mice were maintained under chloral hydrate anesthesia (500 mg/kg) and given one intratracheal injection of bleomycin (1 or 2 mg/kg) to induce fibrosis. Gefitinib (200 mg/kg) was dissolved in 1% methylcellulose and administered orally. GGA (200 mg/kg) was dissolved in 5% arabic gum and 0.06% Tween and administered orally.

Histological analysis

Lung tissue samples were fixed in 4% buffered paraformaldehyde and embedded in paraffin before being cut into 4 μm-thick sections.

For histological examination, sections were stained first with Mayer's haematoxylin and then with 1% eosin alcohol solution. Samples were mounted with malinol and inspected with the aid of an Olympus BX51 microscope.

For Masson's trichrome staining of collagen, sections were sequentially treated with solution A (5% (w/v) potassium dichromate and 5% (w/v) trichloroacetic acid), Weigert's iron hematoxylin, solution B (1.25% (w/v) phosphotungstic acid and 1.25% (w/v) phosphomolybdic acid), 0.75% (w/v) Orange G solution, solution C (0.12% (w/v) xylidine ponceau, 0.04% (w/v) acid fuchsin and 0.02% (w/v) azophloxin), 2.5% (w/v) phosphotungstic acid, and finally aniline blue solution. Samples were mounted with malinol and inspected with the aid of an Olympus BX51 microscope.

Hydroxyproline determination

Hydroxyproline content was determined as previously described [41]. Briefly, the right lung was removed and homogenized in 0.5 ml of 5% TCA. After centrifugation, pellets were hydrolyzed in 0.5 ml of 10 N HCl for 16 h at 110°C. Each sample was incubated for 20 min at room temperature after the addition of 0.5 ml of 1.4% (w/v) chloramine T solution and then incubated at 65°C for 10 min after the addition of 0.5 ml of Ehrlich's reagent (1M DMBA, 70% (v/v) isopropanol and 30% (v/v) perchloric acid). Absorbance was measured at 550 nm and the amount of hydroxyproline was determined.

Statistical analysis

Two-way analysis of variance (ANOVA), followed by the Tukey test or the Student's *t*-test for unpaired results, was used to evaluate differences between more than three groups or between two groups, respectively. Differences were considered to be significant for values of $P<0.05$.

Results

Suppression of expression of HSP70 by gefitinib

We first examined the effects of drugs known to induce ILD clinically (A771726 (an active metabolite of leflunomide), amiodarone, gefitinib and imatinib) on the expression of HSP70 in cultured human type II alveolar (A549) cells. As shown in Fig. S1, a decrease in the level of HSP70 was observed in cells treated with gefitinib but not in cells treated with other drugs.